Sequestration of Carbon in Saline Aquifers

—

Mathematical and Numerical Analysis

Doctor Scientiarum Thesis

Jan Martin Nordbotten

Department of Mathematics
University of Bergen

January 2004

Sequestration of Carbon in Saline Aquifers;
Mathematical and Numerical Analysis

Jan Martin Nordbotten

January 2004
ISBN 82-92160-25-6

Abstract

The work in this thesis focuses equally on two main topics. The first of these subjects deals with development of criteria for monotonicity of control volume methods. These methods are important and frequently used for solving the pressure equation arising in porous media flow. First we consider homogeneous parallelogram grids, and subsequently general logical Cartesian grids in hetrogeneous media. This subject is concluded by the development of a new class of Multi Point Flux Approximation methods, motivated by the monotonicity results obtained.

The second topic of this thesis is the development of analytical and semi-analytical solutions to the problem of leakage through abandoned wells. More specifically, we look at a set of aquifers, separated by impermeable layers (aquicludes), where injection of water or CO_2 takes place in some or all the aquifers. The aquifers and aquicludes are frequently penetrated by abandoned wells from oil exploration, and our problem consists of finding solutions to flow and leakage through these wells. The goal is to obtain expressions for leakage rates that may be evaluated quickly enough such that Monte Carlo realizations over statistical distributions of properties for abandoned wells can be performed.

Acknowledgements

This work is funded by the Norwegian Research Council and Norsk Hydro through Grant 151400/210.

During my doctorate studies, I have had the fortune of being surrounded by many genuinely friendly and helpful people. It is a great honor to have the opportunity to mention a few of these people here.

My thanks go to Magne Espedal, Helge Dahle and Ivar Aavatsmark, who have shared their knowledge and experience with me, and brought me in contact with interesting research communities.

It has been a great pleasure to work with Michael Celia and Stefan Bachu. In their company I always feel welcome, and when working together, new challenges never fail to appear.

Without doubt, Geir Terje Eigestad is the most enthusiastic person I have ever worked with. His common sense view of life makes him not just a fine collaborator, but also a enjoyable lunch partner.

During breaks, it has never been a problem to find relaxing conversation, and for this I am grateful to the graduate students at the mathematics department in Bergen, environmental engineering department in Princeton, and petroleum engineering department in Stanford.

This acknowledgement can not be complete without the mention of Bergen Tuba Quartet, Eikanger-Bjørsvik Musikklag, and all the friends I have met while playing tuba. It is invaluable to have friends in environments where mathematics is nothing more than any other job.

I am also lucky to have a lovely girlfriend. She is a constant reminder that life is more than just numbers. Thank you Linda.

Finally, I thank my parents. Words can never fully express my gratitude to them.

Jan Martin Nordbotten
Bergen, January 2004

Contents

Outline of Thesis **iii**

Acknowledgements **v**

Contents **vii**

Part I

1 Introduction **3**
- 1.1 Geological Sequestration 4
- 1.2 Contribution of this Thesis 5
- 1.3 Structure of Thesis 6

2 Mathematical Model **7**
- 2.1 Material Properties 8
- 2.2 Mass Conservation 8
- 2.3 Darcy's Law 9
- 2.4 Ideal Fluids and Elastic Materials 11
- 2.5 Multi-Fluid Flow 12
- 2.6 General Modeling of CO_2 Flow 13

3 Large Scale Simulation **15**
- 3.1 Athena 16
- 3.2 The Utsira Formation 17

4 Solutions of the Pressure Equation **19**
4.1 Solving the Pressure Equation 20
4.2 Discrete Solutions 20
4.3 Monotonicity 22
4.4 Monotonicity and the MPFA method 26
4.5 The MPFA Z-method 28
4.6 Monotonicity on Quadrilateral Grids 30

5 Semi-Analytical Solutions **33**
5.1 The Alberta Basin 34
5.2 Governing Equations 35
5.3 Brine Leakage from Abandoned Wells 37
5.4 CO_2 Plume Evolution 39
5.5 CO_2 Leakage from Abandoned Wells 41

6 Summary of Papers **45**
6.1 Paper A 46
6.2 Paper B 47
6.3 Paper C 48
6.4 Paper D 49
6.5 Paper E 51
6.6 Paper F 53

7 Further Research **55**
7.1 Monotone Discrete Operators 56
7.2 Leakage from Abandoned Wells 56

Bibliography **59**

Part II

J.M. Nordbotten *and* I. Aavatsmark
Monotonicity Conditions for Control Volume Methods on Uniform Parallelogram Grids in Homogeneous Media . . . . . Paper A

J.M. Nordbotten *and* G.T. Eigestad
Monotonicity Conditions for Control Volume Methods on General Quadrilateral Grids; Application to MPFA . . . . . Paper B
Discretization on Quadrilateral Grids with Improved Monotonicity Properties . . . . . Paper C

J.M. Nordbotten, M.A. Celia *and* S. Bachu
Analytical Solutions for Leakage Rates Through Abandoned Wells . Paper D
Injection and Storage of CO_2 in Deep Saline Aquifers: Analytical Solution for CO_2Plume Evolution During Injection . . . . . Paper E

J.M. Nordbotten, M.A. Celia, S. Bachu *and* H.K. Dahle
Semi-Analytical Solution for CO_2 Leakage through an Abandoned Well . . . . . Paper F

Part I

Chapter 1

Introduction

The earth's climate has been monitored systematically since the middle of the nineteenth century. During this period, numerous variations in our environment have been observed. Amongst the most prominent changes are the shift in mean global temperature, and the carbon dioxide (CO_2) concentration in the atmosphere [36].

It seems certain that the change in CO_2 concentration in the atmosphere is due to human energy production from fossil fuels (e.g. [5]). However, the observed temperature variation is within what can be caused by natural (non-human) processes. The belief that there is a cause and effect relationship between the CO_2 concentration in the atmosphere and global temperatures has lead to much research and international political debate. The global warming issue has sparked public interest on all levels, from multinational environmental organizations, such as Environmental Defense and Greenpeace, to student magazines [43].

To reduce CO_2 emissions, one must either reduce CO_2 production, or find alternative disposal schemes. Due to the important position of fossil fuels in western economies, sequestration of carbon has become an important research topic.

1.1 Geological Sequestration

Several different sequestration schemes have been proposed to reduce atmospheric emissions [56]. Among the most important options are injection into deep oceans, un-minable coal seams, depleted oil reservoirs and saline aquifers. Of these options, storage in deep saline aquifers appears to be the best choice in terms of resident storage time, storage capacity and proximity to emission cites [56].

An extensive introduction to storage of CO_2 in deep saline aquifers can be found in [16]. Some of their main points are:

- The aquifers considered for storage are currently filled with brine (water with high contents of dissolved solids). Brine has little or no economic or social value since it is unfit for both drinking and agricultural purposes.

- The potential storage capacity is vast, estimates vary between 10 and 200 $TtCO_2$ (trillion tons CO_2). Current global emissions are in comparison on the size order of 30 $GtCO_2$ (billion tons CO_2) per year. When economical and technological constraints are included in the storage analysis, capacity is estimated between 200 and 500 $GtCO_2$. Though this amount is significantly smaller than the total capacity, it is still sufficient for 8 – 16 years of global emissions.

- As CO_2 is dissolved in water, the density of water increases. Thus water with dissolved CO_2 will sink relative to the surrounding water, and upward leakage of CO_2 is limited to migration with regional flows.

- Dissolved CO_2 in the water phase will change the equilibrium between brine and the minerals in the surrounding rock. Chemical reactions may occur which have a potential to mineralize CO_2 and change the flow properties of the rock.

- When the CO_2 is injected as a pure phase, the pressure and temperature regimes imply that it is supercritical. Supercritical CO_2 under these conditions is much denser than CO_2 in gaseous phase, but still less dense than water. The buoyancy of CO_2 will drive it upwards, thus creating a potential for leakage.

- Leakage to the surface may occur through geological fractures and faults in the confining layers and through abandoned wells from oil exploration and production.

Several research questions arise from the above. It is of general interest to determine the storage capacity more precisely and enhance technology and economic viability of CO_2 sequestration schemes. It is also important to determine the rate at which CO_2 dissolves into the water phase, since this determines the amount of carbon which is safely sequestered. Herein we focus on determining the extent of CO_2 migration and leakage.

1.2 Contribution of this Thesis

This thesis contributes with both numerical analysis and analytical studies.

The Multi Point Flux Approximation (MPFA) methods [1, 3] were introduced as a solution to the pressure equation with direct expressions for fluxes. The methods have since been developed in several papers (for example, five articles in the special issue of *Computational Geosciences* on locally conservative methods [27]). However, the methods do not necessarily have monotone inverse operators even on parallelogram grids [1]. This thesis develops criteria for monotonicity of the inverse operator on regular parallelogram grids on homogeneous media in Paper A, which are valid for nine-point discretization methods. In Paper B, these criteria are extended to general logical Cartesian grids. Further, for the particular case of the MPFA methods, a set of homogeneous parallelogram grids were discovered for which none of the existing MPFA methods have a positive inverse operator. This motivates the development of a new MPFA method in Paper C, which is shown to have better monotonicity properties. The new method is shown to converge at the same rate as the classical MPFA methods in a numerical example.

Single-fluid flow to a well has been described by Theis [55] for confined homogeneous aquifers, and for systems of multiple aquifers and aquitards (slightly permeable layers) by e.g. [37]. However, in the case of injection, leakage may occur not only through the aquitards but also through abandoned wells from oil exploration [16]. This has been investigated in the case of two aquifers with aquicludes (impermeable layers) above, below and between, and connected by a single abandoned well for a single fluid in [8]. Even in this simple case an analytical solution can not be obtained due to the complexities arising from a convolution integral. This thesis simplifies the convolution integral and manages to find solutions for single-fluid systems with an arbitrary number of aquifers and abandoned wells. These developments are presented in Paper D. One may consider the Cooper-Jacob solution for well testing [11] as equivalent to approximating the parabolic pressure equation with a steady state (elliptic) equation on a time-expanding domain. Paper

E uses this observation together with arguments of minimization of energy to obtain an expression for the CO_2 plume during injection. This solution is shown to be valid for even the most extreme pressure and temperature regimes one expects to encounter in CO_2 sequestration projects. This is combined with some of the single-fluid work, and in Paper F an expression for two-fluid leakage, corresponding to CO_2 and brine, through an abandoned well for a system with multiple aquifers is obtained.

Thus the material in this thesis has been developed in a total of six manuscripts, of which one is published in a conference proceeding, while the remaining five are currently under journal review. These manuscripts are reproduced in full in Part II of this thesis. The manuscripts have been completed in collaboration with co-authors. In general, this author's contribution has been the development and testing of solution techniques, while motivation, problem formulation and writing have been collaborative between all the authors.

1.3 Structure of Thesis

An introduction and general motivation for the CO_2 sequestration problem is provided in Chapter 1 of Part I. Chapter 2 introduces the mathematical models and notation used to represent the injection and flow problems media that we consider. Numerical solutions of these models are used in validating our analytical and semi-analytical solutions. Chapter 3 provides a brief overview of the development of a numerical simulator which uses the Multi Point Flux Approximation (MPFA) method to solve the pressure equation. Chapter 4 introduces work presented in the manuscripts on the monotonicity of Control Volume methods. Chapter 5 motivates and develops analytical and semi-analytical solutions of the coupled parabolic equations modeling CO_2 injection under certain simplifications. The abstracts of the papers in Part II, as well as statements regarding the main results of these papers are given in Chapter 6. General conclusions drawn from all the work in this thesis, along with some ideas for future research are presented in the final chapter.

Chapter 2

Mathematical Model

Our goal is to describe the motion of injected CO_2 in an aquifer. The fluid flow (both water and supercritical CO_2) will be dependent not only on their individual properties, but also on the properties of the surrounding medium. These properties are in general dependent on variables, such as temperature and pressure, and may also vary when chemical reactions occur.

This chapter will introduce the mathematical preliminaries of multi-fluid flow. We will use a consistent multi-fluid notation throughout the introductory part of the thesis, although a different notation is adopted in several of the papers in part II. The theory in this chapter is analogous to that which may be found in most textbooks on porous media flow, e.g. [11] or [33].

2.1 Material Properties

We will concern ourselves with at most two fluids and a solid matrix. By solid matrix we understand a porous medium, in particular compacted sediments at depths greater than one kilometer below the surface. Associated with the solid matrix are numerous physical properties, of which the porosity and permeability will be of main interest. The nature of these properties will be explained later.

The fluids in our system are brine (water with high concentrations of dissolved minerals) and CO_2. The subsurface conditions that are relevant to CO_2 injection are described in Paper E. In these ranges of pressure and temperature, the CO_2 will be supercritical. A fluid is said to be supercritical when the pressure and temperature is above the critical point of the fluid [32]. The critical point is the highest temperature and pressure in which the fluid can exist both as a gas and a liquid simultaneously. The supercritical region provides a continuous phase transition from gas to liquid.

Fluid properties for water and CO_2 at appropriate pressure, temperature and salinity conditions can be found in e.g. [4] and [54]. We will only briefly discuss CO_2-water phase equilibria, and for the most part treat CO_2 and water as separate fluids.

2.2 Mass Conservation

Physically, a fluid consists of molecules with a certain mass and spacing between them. Macroscopically, we talk about fluid particles, which are understood to be infinitesimal volumes in respect to the length scales we are concerned with, yet large enough so that a molecule is infinitesimal in respect to the fluid particle. With a particle we may associate a density ρ, which may be defined as the average molecule mass divided by average molecule spacing

$$\rho(\boldsymbol{x}, t) = \lim_{V(\boldsymbol{x},t)\to 0} \frac{M(V(\boldsymbol{x}, t))}{V(\boldsymbol{x}, t)}. \tag{2.1}$$

In this definition, $V(\boldsymbol{x}, t)$ is a macroscopic volume enclosing the point $(\boldsymbol{x}, t)$ in space and time, while M is the mass contained within the volume.

The basic principle used to develop governing equations for single-fluid flow is the conservation of mass. This can be written in the Lagrangian formulation as

$$\int_{V(t_1)} \phi(\boldsymbol{x}, t_1)\rho(\boldsymbol{x}, t_1)d\boldsymbol{x} = \int_{V(t_2)} \phi(\boldsymbol{x}, t_2)\rho(\boldsymbol{x}, t_2)d\boldsymbol{x}, \tag{2.2}$$

where $V(t_2)$ is the volume spanning the same set of fluid particles at time t_2 as $V(t_1)$ did at t_1. The porosity, $\phi(\boldsymbol{x}, t)$, indicates the fraction of the volume which is available for fluid flow. Typically, the rock occupies the remaining $(1 - \phi)$ fraction of the volume. For computational purposes, it is often convenient to use the Eulerian description. A coordinate transformation and differentiation with respect to time of Equation (2.2) leads to

$$\int_V \frac{\partial}{\partial t}(\phi\rho)d\boldsymbol{x} + \int_{\partial V} \rho\boldsymbol{q} \cdot \boldsymbol{n}d\boldsymbol{x} = \int_V Qd\boldsymbol{x}. \tag{2.3}$$

The volume V is now fixed in space, its surface is denoted ∂V, and the outward normal vector of this surface is $\boldsymbol{n}$. Further, $\boldsymbol{q}$ indicates the macroscopic flux of the fluid, and Q is some source or sink term, usually due to injection or production of the fluid. The flux is a measure of volume flowing through a surface per time. As such it can be related to the flow velocity $\boldsymbol{v}$ by $\boldsymbol{v}\phi = \boldsymbol{q}$, under the understanding that areal porosity is equal to the volumetric porosity [25]. Equation (2.3) can be expressed locally by applying the divergence theorem to the second term and using the fact that the equation is valid independent of integration volume:

$$\frac{\partial}{\partial t}(\phi\rho) + \nabla \cdot (\rho\boldsymbol{q}) - Q = 0. \tag{2.4}$$

In cases where the fluid and the solid matrix may be considered incompressible, the local (in space and time) form of Equation (2.2) states that

$$\frac{\partial}{\partial t}(\phi\rho) + \boldsymbol{q} \cdot \nabla\rho = 0, \tag{2.5}$$

which combined with Equation (2.4) reduces to

$$\rho\nabla \cdot \boldsymbol{q} - Q = 0. \tag{2.6}$$

2.3 Darcy's Law

As with Newton's second law of motion, Darcy's law [24] is a relationship between force and movement. When in free space, as observed by Newton, the acceleration is proportional to force. However, when opposing forces such as air resistance are present the velocity approaches a critical velocity (for a given force), above which it will not accelerate. This is also the case of fluids in porous media, and Darcy's law can be interpreted to state that this critical velocity is quickly reached, and moreover, the critical velocity is proportional to the forces acting on the fluid particles. Mathematical justification for

this macroscopic relationship can be found by volume averaging pore-scale Navier-Stokes equations [47]. Still considering single-fluid flow, and using flux instead of velocity, Darcy's law is stated as

$$\boldsymbol{q} = -\frac{\boldsymbol{K}}{\mu}(\nabla p + \rho g \nabla d). \tag{2.7}$$

The terms in the parenthesis represent the forces per volume acting on the fluid particle, in particular the pressure gradient (∇p) and gravitational force in the d-direction. The matrix $\boldsymbol{K}$ is referred to as the permeability, and is an empirical determined quantity of the porous medium. The permeability is scaled by the viscosity μ, which is the internal resistance to flow in the fluid.

Sometimes it is appropriate to consider the fluid and solid matrix as incompressible. If this is the case, we may combine Equation (2.7) with Equation (2.6), and assuming homogenous density in the fluid we obtain

$$-\nabla \cdot \left(\frac{\boldsymbol{K}}{\mu}\nabla p\right) = \frac{Q}{\rho}. \tag{2.8}$$

We recognize this to be an elliptic equation, containing no time dependency. Solutions of this equation will frequently be referred to as steady state solutions. In the case of an isotropic homogenous medium, $\boldsymbol{K}$ will be a constant scalar K, and with constant viscosity Equation (2.8) reduces to the Laplacian equation. On an infinite two-dimensional domain when Q is a point source the solution of Equation (2.8) is

$$p = -\frac{Q\mu}{2\pi K\rho}\ln|\boldsymbol{x} - \boldsymbol{x}_Q| + C \tag{2.9}$$

where C is some constant dependent on the outer boundary, and $\boldsymbol{x}_Q$ is the position of the source. Throughout this thesis $|\cdot|$ will be understood to mean the Euclidian distance. We note that for finite C, this solution extends from plus to minus infinity. In practice we limit the domain by an outer boundary and an inner radius (the radius of the well), which ensures that the solution is finite. Under appropriate smoothness conditions and zero pressure boundary conditions, Equation (2.8) has the solution [35]

$$p(\boldsymbol{x}) = \int_\Omega Q(\boldsymbol{\xi})G(\boldsymbol{x},\boldsymbol{\xi})d\boldsymbol{\xi}. \tag{2.10}$$

The Green's function G (see e.g. [29]) is dependent on the domain and is for general domains impossible to find analytically. Corresponding to the solution for a simple domain given in Equation (2.9), we see that the appropriate Green's function in Equation (2.10) is given by

$$G = -\frac{Q\mu}{2\pi K\rho} \ln |\boldsymbol{x} - \boldsymbol{\xi}|. \tag{2.11}$$

Equation (2.8) and its solution are important in reservoir modeling, since they provide an equation relating the pressure to flux. However the assumption that the fluid and solid matrix are incompressible means that density and porosity variations must be accounted for through boundary terms or the source function. This will be discussed further in Chapters 4 and 5.

Often it is better to include compressibilities directly into the differential equation. To do this, we need to introduce ideal fluids and elastic materials.

2.4 Ideal Fluids and Elastic Materials

As was noted in the conclusion of the previous section, the solution of the elliptic equation leads to infinite pressures on domains of infinite extent. Further, there is no time component due to the elimination of density variation in Equation (2.4). The simplest way to incorporate density variation, is by assuming that the fluid behaves like an ideal fluid and that the rock is elastic.

An ideal fluid is a fluid in which the internal viscous forces are negligible. Empirically, it has been observed that in these fluids compressibility c_f may be defined as

$$c_f = \frac{1}{\rho}\frac{\mathrm{d}\rho}{\mathrm{d}p}. \tag{2.12}$$

Within the region where compressibility can be assumed constant, fluid density is related to pressure through

$$\rho = \rho_0 \mathrm{e}^{c_f(p-p_0)}, \tag{2.13}$$

where ρ_0 is the initial density. With elastic representation of the solid matrix, the porosity ϕ varies linearly with pressure [19], so that we may write

$$\phi = \phi_0 + c_r(p - p_0). \tag{2.14}$$

where c_r is the compressibility coefficient for the porosity. By combining equations (2.4), (2.7), (2.13) and (2.14), we obtain the basic equation for transient flow in porous media:

$$(c_f\phi + c_r)\rho\frac{\partial}{\partial t}p - \nabla \cdot \left(\rho\frac{\boldsymbol{K}}{\mu}(\nabla p + \rho g \nabla d)\right) - Q = 0. \tag{2.15}$$

We linearize this equation with respect to pressure by inserting Taylor expansions around p_0 of equations (2.13) and (2.14), keeping only the lowest order (constant) terms. We have now arrived at the pressure equation

$$(c_f\phi_0 + c_r)\frac{\partial}{\partial t}p - \nabla\cdot\left(\frac{\boldsymbol{K}}{\mu}\nabla p + \rho_0 g\nabla d\right) - \frac{Q}{\rho_0} = 0. \tag{2.16}$$

The difference between fluid and matrix compressibility will not be important in this work, and we therefore use the total compressibility $c = c_f\phi_0 + c_r$ instead. Equation (2.16) is parabolic, and is identical in structure to the heat equation. The solution of Equation (2.16) for isotropic and homogenous $\boldsymbol{K}$ and constant viscosity is frequently referred to as the Theis solution [55]:

$$p(\boldsymbol{x}) - p_{init} = -\frac{Q\mu}{4\pi K\rho_0}\int_u^\infty \frac{e^{-x}}{x}dx, \tag{2.17}$$
$$u = \frac{c\mu|\boldsymbol{x} - \boldsymbol{x}_Q|^2}{4Kt}.$$

This solution assumes a domain which is either two-dimensional and in the horizontal plane, or a three dimensional domain where the source term Q is a line source penetrating the entire aquifer and where the aquifer has constant thickness. In the latter case p and Q should be thought of as vertically averaged.

Note that the Theis solution implies that pressure increases instantaneously at all points in the domain as a response to injection. As time goes to infinity, the pressure will also approach infinity at every point in the domain. The instantaneous propagation of information is an indication that Equation (2.16) does not capture all the physics of the system.

By a series expansion of Equation (2.17) we can obtain boundary and source terms for the elliptic Equation (2.8) which approximate compressibility. This turns out to be important, and will be discussed in more detail in Chapter 5.

2.5 Multi-Fluid Flow

The previous sections have been devoted to single fluid flow. To model the flow patterns of CO_2 and water in sequestration scenarios, we will review the governing equations for two fluids. The simplest formulation is obtained by assuming that the fluids are immiscible.

Under the assumption that Darcy's law is valid independently for each fluid, mass conservation can be formulated as [28]

$$\frac{\partial \phi \rho_i S_i}{\partial t} - \nabla \cdot \left(\rho_i \frac{\boldsymbol{K} k_{r,i}}{\mu_i} (\nabla p + \rho_i g \nabla d) \right) = 0 \qquad i = c,\, w. \tag{2.18}$$

We have introduced the fluid saturation S_i and the relative permeability $k_{r,i}$ for the two fluids (**c**arbon and **w**ater). The pressure p is the fluid pressure for both fluids, which corresponds to an assumption of zero capillary pressure. Also, in this model phase transitions or chemical reactions are not considered.

The relative permeability is a scaling of the intrinsic permeability reflecting that there are two fluids competing for the pore-space. The relative permeability always serves to reduce the permeability, hence it takes values between zero and one. The functional form of $k_{r,i}$ is the topic of much research, network modeling of porescale processes such as relative permeability is described in [13] and references therein. In this work we use the common assumption that relative permeability is a function of saturation only, $k_{r,i} = k_{r,i}(S_i)$.

When relative permeability is a function of saturation, density is a function of pressure (e.g. as in the single-fluid discussion), and also the material properties porosity and viscosity are known functions of pressure, then equations (2.18) only contains three unknowns. These are the pressure, and the two saturations. We have assumed that only two fluids are present in the flow, and these fluids must then fill the pore space,

$$S_c + S_w = 1. \tag{2.19}$$

Equations (2.18) along with (2.19) form a closed system of equations.

2.6 General Modeling of CO_2 Flow

There are several potentially important features of CO_2 injection which are not captured in the models of the preceeding sections. We will briefly review some of the most interesting features in this section.

When supercritical CO_2 comes in contact with water, the fluids are not immiscible. The CO_2 has a capacity to absorb some water (which may dry up residual water), while a significant amount of CO_2 can dissolve into the water phase [6, 22]. The dissolution of CO_2 can only occur at the boundary between the two phases, thus the effective rate of dissolution may be dependent on the diffusion of CO_2 through the water phase.

Complicating the dissolution process is the fact that CO_2-saturated water is denser than undersaturated water. Since separate phase CO_2 is primarily at the top of the formation as it is lighter than water, satured and therefore

denser water will accumulate above un-saturated, less dense water. Convectional circulation will occur as the denser water sinks, producing some circulation of un-saturated water to the phase boundary, which may enhance dissolution [41].

Water becomes acidic when CO_2 is dissolved. This shifts the equilibrium between the minerals in the host formation and the fluid. These changes may potentially affect both the porosity and permeability of the medium, thus affecting flow. Typically, only CO_2 dissolved in the water phase will react with minerals.

Mineral reactions are usually associated with changes in internal energy [6], thus thermal effects may be important. Also, as the CO_2 migrates in the vertical direction, the background temperature changes. Thus incorporating heat transfer and temperature dependence of the variables may be important.

From these observations we conclude that a thermal compositional reactive transport model may be necessary to fully resolve the processes involved in CO_2 injection schemes in realistic aquifers. For descriptions of such models, see e.g. [20, 21]. The CO_2 storage project in Bergen is developing its own simulator Athena, which will be described in the next chapter.

Chapter 3

Large Scale Simulation

In this chapter we will review the solution procedure implemented in the basin simulator Athena as an example of a numerical solution to the models presented in Chapter 2. We will also give a brief review of the injection activities into the Utsira formation as a field example.

Numerical simulators such as Athena are important in most of the work in this thesis. The analytical and semi-analytical solutions will be compared directly against the output from numerical simulators, since some numerical simulators are known to be stable and convergent [53]. The work done in this thesis on monotonicity has direct implications to the output from simulators using Control Volume methods, such as Athena.

3.1 Athena

As noted in Section 2.6, a thermal compositional reactive transport model is needed to represent all aspects of CO_2 injection. Athena (also known as Secondary Oil Migration, SOM [31]) was chosen to simulate such a model, although it did not have any reaction terms implemented. In its current form, versions of Athena are capable of

- Multi-component, multi-phase thermal transport.
- General unstructured, non-matching grids with local grid refinement.
- Parallel processing in space and time.
- Implicit treatment of pressure and transport equations.
- Multi-Point Flux Approximations (MPFA) to the pressure equation.

Details on the implementation of the governing equations can be found in [30], while details on the above features can be found in [18, 45, 46, 48].

As primary variables, Athena uses the temperature, water pressure, and component molar masses in each control volume. For an n_c component system, we therefore need n_c+2 differential equations to close the system. These are conservation of mass (n_c molar mass equations), conservation of internal energy (temperature equation), and a water pressure equation derived from volume balance (pressure equation).

For each control volume, secondary variables include the molar masses in each phase, the pressure in the non-aquas phases, fluid densities and viscosities, internal energy and enthalpy, as well as rock properties such as porosity, permeability and overburden pressure. These are all functions of the primary variables through constitutive relationships.

In each time step

- An implicit temperature equation is solved.
- An implicit pressure equation is solved.
- The molar mass equation and secondary variables are solved and updated.
- An outer iteration is implemented to ensure convergence.

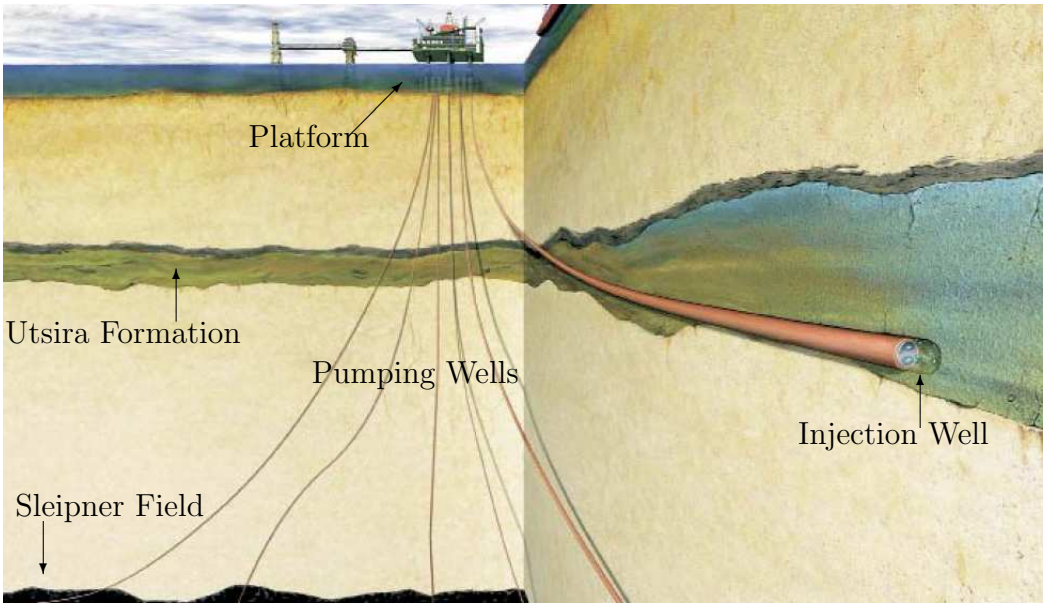

Figure 3.1: An artists rendering of the Utsira injection (figure courtesy of the Norwegian Petroleum Directorate).

3.2 The Utsira Formation

The Sleipner field was discovered in 1974, and has since 1996 been producing gas. The composition of the produced gas contains about 9% CO_2 [50]. With current production rates of 2800 metric tons of CO_2 per day [44] and the environmental taxes enforced by the Norwegian government, the cost of releasing the CO_2 into the atmosphere would amount to around one million Norwegian kroner (NOK) per day [42]. It was therefore decided by the operator (Statoil) that the CO_2 should be sequestrated in the Utsira formation.

The Utsira formation itself is located above the Sleipner field, at about 800 – 1000 meters below sea level. The formation spans some 26000 square kilometers, and has a pore volume of approximately 550 billion cubic meters. With CO_2 storage capacity of water of approximately 50 kg CO_2 per cubic meter [9], the formation has a theoretical storage capacity for around 30 thousand years of injection from the Sleipner field. Even though the realistic storage capacity will only be a fraction of this number, the Utsira formation has an enormous potential for sequestration.

Injection into Utsira started simultaneously with the production of gas from Sleipner. To monitor the sequestered CO_2, a research collaboration was initiated between the participating oil companies and the neighboring

nations. This collaboration, Saline Aquifer CO_2 Storage (SACS) [50], has monitored the injection from injection start up to the year 2000. Their conclusion was that no trace of leakage from the formation could be detected.

Our project focuses on long term migration and storage of CO_2, and aims at incorporating realistic CO_2 dissolution rates, as well as accurate representations of mineral reactions. We plan on using the Utsira as a field case for our simulator, since this is a case well established in literature, with real life data available. Also, as injection activities are currently operating, this site is a direct practical application with social, economical and political importance. As the Norwegian government also plans on injecting into the Tubåsen formation (associated with production from Snøhvit), it is a project goal that simulations from Athena can be used in analyzing the safety of CO_2 injection into Tubåsen.

Chapter 4

Solutions of the Pressure Equation

For general boundary conditions and coefficients, analytical solutions of the pressure equation do not exist. We therefore have to rely on numerical methods which require that the variables are discretized in space and time. We will focus our attention on a particular class of numerical methods, and investigate their monotonicity properties. This work will lead to the development of a new discretization method.

4.1 Solving the Pressure Equation

Throughout this chapter we consider only the single-fluid pressure equation, since the structure of the pressure equation is mathematically similar to the multi-fluid equivalents, but simpler with respect to notation, as can be seen by comparing Equation (2.16) with the pressure equation used in e.g. [28].

Writing Equation (2.16) with a discrete representation of time and a first order finite difference representation of the time derivative leads to

$$c\phi_0 \frac{1}{\delta t}(p^{t+1} - p^t) - \nabla \cdot (\frac{\boldsymbol{K}}{\mu}\nabla p^\tau + \rho_0 g \nabla d) - \frac{Q^\tau}{\rho_0} = 0. \tag{4.1}$$

The superscripts t and $t+1$ indicate the discrete time levels, and we recognize that the choice of $\tau = t$ or $\tau = t+1$ leads to an explicit or implicit method, respectively. As an example, the explicit formulation can be written

$$p^{t+1} = p^t + \frac{\delta t}{c\phi_0}(\nabla \cdot (\frac{\boldsymbol{K}}{\mu}\nabla p^t + \rho_0 g \nabla d) + \frac{Q^t}{\rho_0}). \tag{4.2}$$

The implicit formulation does not have a direct expression for the pressure at the new time step.

To obtain a finite number of unknowns, the spacial coordinates must also be discretized. We immediately see from Equation (4.2) that we need a discrete representation of the operator $[-\nabla \cdot (\boldsymbol{K}\nabla \bullet)]$ for discontinuous and anisotropic $\boldsymbol{K}$. This operator is the same operator as in Equation (2.8), and discretizing the operator $[-\nabla \cdot (\boldsymbol{K}\nabla \bullet)]$ is therefore equivalent to discretizing an elliptic equation.

The numerical solution of elliptic equations is a problem that is still under extensive research. Common methods include the Mixed Finite Element method (MFE) [15], the Support Operators method (SO) [38], Enhanced Cell-Centered Finite Differences (ECCFD) [7] and the Multi Point Flux Approximation control volume methods (MPFA) [1]. Further, a special issue of Computational Geosciences [27] is devoted to this subject. Thorough comparisons of the most important methods can be found in [40, 49].

4.2 Discrete Solutions

In [49], discretizations of Equation (2.8) are divided into $\boldsymbol{K}$ and $\boldsymbol{K}^{-1}$ methods according to how they represent Equation (2.7). Leaving details aside, $\boldsymbol{K}^{-1}$ methods such as MFE and SO represent pressure drops as a combination of fluxes,

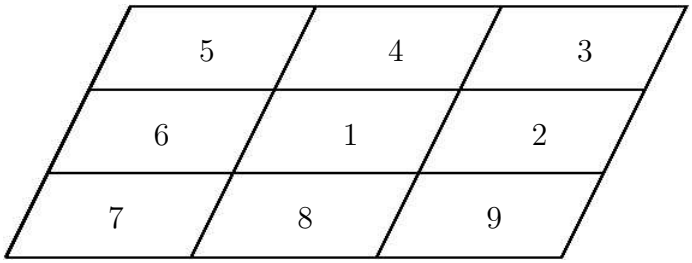

Figure 4.1: Local numbering of cells

$$\nabla p = -\boldsymbol{K}^{-1}\boldsymbol{q}. \tag{4.3}$$

In contrast, the $\boldsymbol{K}$ methods such as ECCFD and MPFA express fluxes in terms of pressure drops,

$$\boldsymbol{q} = -\boldsymbol{K}\nabla p. \tag{4.4}$$

When discretizing Equation (2.8), we then get a relation $\boldsymbol{Ap} = \boldsymbol{Q}$, where $\boldsymbol{p}$ and $\boldsymbol{Q}$ are vectors of integrated pressures and source terms. For $\boldsymbol{K}$ methods $\boldsymbol{A}$ itself is known and sparse while the inverse is a full matrix, conversely $\boldsymbol{A}$ is a full matrix for $\boldsymbol{K}^{-1}$ methods but the inverse is known and sparse. Incomplete inversion of the system matrices $\boldsymbol{A}$ have shown similarities between $\boldsymbol{K}$ and $\boldsymbol{K}^{-1}$ methods [49].

It is known that $\boldsymbol{K}$ methods may have problems with monotonicity [1], and this has been the motivation for the work in this chapter. Before we look at monotonicity, we will give a short outline of $\boldsymbol{K}$ method discretizations. In particular we will look at conservative methods that use nine pressures in two dimensions and 27 pressures in three dimensions, which fall into the class of Control Volume (CV) methods.

Referring to Figure 4.1, quadrilateral nine-point methods in two dimensions use a linear combination of the pressure in the discrete points 1–9 to estimate the total outflow over the boundary of the central cell (the control volume). Similar stencils with 27 points arise for discretizations in three dimensions. This can be seen as an approximation to the operator arising in the integral formulation of Equation (2.8),

$$\mathcal{L}(u) = \int_{CS} (\boldsymbol{K}\nabla u) \cdot \boldsymbol{n} dS. \tag{4.5}$$

The surface of the control volume is termed CS, while $\boldsymbol{n}$ is the outward unit normal vector to this surface. The discrete approximation of (2.8) is for control volume $\boldsymbol{K}$ methods

$$\int_{CV} Q dV = \int_{CS} (\boldsymbol{K}\nabla p) \cdot \boldsymbol{n} dS \approx \sum_{i=1}^{9 \text{ or } 27} m_i p_i. \tag{4.6}$$

Thus the integrated source term associated with a cell is approximated by a linear combination of the pressure in this cell and the surrounding eight cells. Generally, the weights m_i contain implicitly the permeability and physical structure of the grid. The discretization is therefore defined by the logical structure and values of these weights.

Applying such stencils to all cells in a grid with appropriate modifications at the boundary, results in a set of linear equations which can be written in matrix form,

$$\boldsymbol{A}\boldsymbol{p} = \boldsymbol{Q}. \tag{4.7}$$

We refer to $\boldsymbol{A}$ as the system matrix, while $\boldsymbol{p}$ is a vector composed of the discrete pressures and $\boldsymbol{Q}$ is a vector of integrated source and sink terms.

When the system matrix $\boldsymbol{A}$ approximates the operator (4.5), it should ideally share the same properties as the continuous operator. Examples of such properties are (see e.g. [1, 51, 52]):

i) Conservation of mass.

ii) No accumulation for linear pressure variation.

iii) Correct behavior with respect to symmetry.

iv) Monotonicity of inverse operator.

In addition, discrete operators and their inverse should be stable, and the discretization methods should be convergent. Several additional properties, primarily related to computational aspects, may also be of interest for applications [1, 51, 52].

Due to the complications involved in inverting the system matrix, the monotonicity property has gained little attention in the discussion of $\boldsymbol{K}$ methods, even though it is often violated [1, 14, 51]. In the following two sections we will investigate this property on nine-point $\boldsymbol{K}$ methods and in particular the Multi Point Flux Approximation (MPFA) methods.

4.3 Monotonicity

Under appropriate smoothness conditions, Equation (2.8) on a domain Ω can be expressed for p as [35]

$$p(\boldsymbol{x}) = \int_{\Omega} q(\boldsymbol{\xi}) G(\boldsymbol{x}, \boldsymbol{\xi}) \mathrm{d}\boldsymbol{\xi}. \tag{4.8}$$

It is well known that the Green's function G satisfies the maximum principle; thus for zero pressure boundary condition G is monotone [29]. A linear operator $\boldsymbol{L}$ is monotone if either $\boldsymbol{Lx} \leq \boldsymbol{0}$ or $\boldsymbol{Lx} \geq \boldsymbol{0}$ for all $\boldsymbol{x} \geq \boldsymbol{0}$. This can be written as

$$G(\boldsymbol{x}, \boldsymbol{\xi}) \geq 0, \quad \forall\ \boldsymbol{x}, \boldsymbol{\xi}. \tag{4.9}$$

It follows that the inverse of the operator $[-\nabla \cdot (\boldsymbol{K} \nabla \bullet)]$ is monotone.

If a linear operator is represented by a matrix, the operator is monotone if and only if all elements in the matrix have the same sign. Consequently the discrete representation $\boldsymbol{A}$ of Operator (4.5), has a monotone inverse if

$$\boldsymbol{A}^{-1} \geq \boldsymbol{O}. \tag{4.10}$$

By $\boldsymbol{O}$ we understand the zero matrix, and the inequality is interpreted elementwise. The operator is also monotone if the inequality is inverted, however the sign used in Equation (4.10) is chosen to conform with Equation (4.9).

It is well known that inverting matrices is highly time consuming [23]. It is therefore desirable to develop methods for determining monotonicity of the inverse operator without inverting the system matrix.

In idealized cases, some $\boldsymbol{K}$ methods produce matrices that are M-matrices. An M-matrix is a matrix for which the entries satisfy [12]

$$\begin{array}{lll} a_{i,i} > 0, & \forall\, i, & \\ a_{i,j} \leq 0, & \forall\, i, j, & i \neq j, \\ \sum_i d_i a_{i,j} \geq 0, & \forall\, j, & \end{array} \tag{4.11}$$

for some positive vector $\boldsymbol{d}$. M-matrices can easily be shown to have monotone inverses [12]. Standard 5-point discretization stencils (consisting of the points 1, 2, 4, 6, and 8 in Figure 4.1) usually yield M-matrices [1]. The same holds for 7-point stencils in three dimensions. However, the condition that the system matrix must be an M-matrix in order to have a monotone inverse, is often too restrictive when dealing with 9-point and 27-point stencils [1].

In Paper A, 9-point stencils arising from $\boldsymbol{K}$ method discretizations are investigated. It is shown that on uniform parallelogram grids in a two dimensional homogenous media, the following theorem is valid with m_i defined in Equation (4.6).

Theorem 1 (Monotonicity on uniform grids)

The inverse of the matrix $\boldsymbol{A}$ *generated from a 9-point discretization of the operator* $[-\nabla \cdot (\boldsymbol{K}\nabla\bullet)]$ *in two dimensions, is monotone if the following sufficient criteria are satisfied:*

$$\begin{aligned}
&\textit{(C1):}\ -m_2 = -m_6 < m_1/2,\\
&\textit{(C2):}\quad m_2 = m_6 < 0,\\
&\textit{(C3a):}\ m_2 \cdot m_4 - m_3 \cdot m_1 \geq 0,\\
&\textit{(C3b):}\ m_2 \cdot m_4 - m_5 \cdot m_1 \geq 0.
\end{aligned}$$

The proof is given in Paper A, and is based on building a series of approximations to the inverse matrix, which are positive when criteria C1 – C3 are fulfilled. This series of approximations is shown to converge to the inverse matrix, hence the inverse matrix must also be positive. We emphasize that these criteria are only sufficient for monotonicity.

For less regular grids, criteria C1 – C3 do not apply. For such grids evaluating monotonicity becomes more difficult. While 9-point discretizations are local formulations, the monotonicity property of the inverse is global in nature, since the inverse matrix is a full matrix. Therefore, on irregular grids, we have focused on finding ways of evaluating monotonicity faster than inverting the full banded matrix.

Inspired by the proof of Theorem 1, Paper B introduced the matrix splitting

$$\boldsymbol{A} = (\boldsymbol{A}\boldsymbol{A}_3^{-1})\boldsymbol{A}_3. \tag{4.12}$$

Here $\boldsymbol{A}_3$ refers to the matrix consisting of the leading tridiagonal matrix of $\boldsymbol{A}$. It is assumed that the grid is logically Cartesian, and that a natural cell numbering is used. The following lemma follows immediately from inverting Equation (4.12).

Lemma 1 (Monotonicity on general grids)

The inverse of the matrix $\boldsymbol{A}$ *generated from a 9-point discretization of the operator* $[-\nabla\cdot(\boldsymbol{K}\nabla\bullet)]$ *in two dimensions, on a general quadrilateral grid, is monotone if the following sufficient criteria are satisfied:*

$$\begin{aligned}
&\textit{(D1):}\ \boldsymbol{A}_3^{-1} \geq \boldsymbol{O}.\\
&\textit{(D2):}\ (\boldsymbol{A}\boldsymbol{A}_3^{-1})\ \textit{is an M-matrix.}
\end{aligned}$$

It is shown in Paper B that for an $m \times n$ grid, the cost of evaluating criteria D1 and D2 is of order $O(m^2 n)$, while inverting the full matrix requires

$O(m^2n^2)$ operations. Thus on large grids, a significant reduction of computational cost is inferred. When the grids become highly distorted, it turns out that Criterion D2 is too restrictive. An approximate criterion can be obtained from the insight that matrices which are close to being M-matrices tend to have positive inverses, thus in Paper B Criterion D2 is relaxed to the following practical criterion.

> (D2c): Less than 9% of the off diagonal elements of $(\boldsymbol{A}\boldsymbol{A}_3^{-1})$ are positive.

Even though D2c is no longer a sufficient criterion, it has shown good results for the MPFA O-method.

To show the equivalence between criteria C1 – C3 and Criterion D1 and D2, we will now prove Theorem 1 using Lemma 1. Notation from papers A and B will be used without further introduction.

> *Proof of Theorem 1:* On a uniform $n \times m$ parallelogram grid in a homogenous medium, local symmetry implies that the system matrix $\boldsymbol{A}$ is symmetric. The matrix $\boldsymbol{A}_3$ consists of m identical tridiagonal $n \times n$ matrices. Denote such an $n \times n$ matrix $\boldsymbol{B}$. The tridiagonal matrix $\boldsymbol{B}$ has the elements m_1 on the leading diagonal and m_2 and m_6 on the off-diagonals. For tridiagonal matrices where the elements on each band are fixed, the inverse matrix is positive if and only if the matrix is an M-matrix, as can be inferred from Equation (12) in Paper A. Referring to the definition of an M-matrix, we therefore see that: *Criteria C1 and C2 are equivalent to criterion D1.*
>
> Interpreting the 1D Green's function $G_{n,1}^{n,1}$ as a vector, Equation (11) from Paper F can be written
>
> $$\boldsymbol{B}G_{n,1}^{n,1} = \boldsymbol{\delta}_n \tag{4.13}$$
>
> where $\boldsymbol{\delta}_n$ is the vector $[\overbrace{0, 0 \dots 0}^{n-1}, 1]^T$. Thus, if we define the matrix $\boldsymbol{G} = [G_{n,1}^{1,1}, G_{n,1}^{2,1}, \dots, G_{n,1}^{n,1}]$, we see that
>
> $$\boldsymbol{B}^{-1} = \boldsymbol{G}. \tag{4.14}$$
>
> Observe from this equation that the product $\boldsymbol{A}\boldsymbol{A}_3^{-1}$ equals the operator F from Paper A applied to the pressure distributions represented by $\boldsymbol{G}$. Thus, the expression $F(H_{n,m}^{r,s}, a, b)$ of Criterion

C3 in Paper A equals the element $[(b-1)n+a,(s-1)n+r]$ in the matrix $\boldsymbol{A}\boldsymbol{A}_3^{-1}$. Therefore, *Criterion D2 implies Criterion C3.* The reverse implication follows directly by comparing Criterion C3 and Inequality (26) in Paper A to the definition of an M-matrix. □

The above proof shows that the matrix criteria D1 and D2 are natural extensions of criteria C1 – C3 to irregular grids. Criteria D1 and D2 themselves may further be extended to three dimensions. With the notation that $\boldsymbol{A}_{2n+3}$ is the matrix containing the $2n+3$ leading diagonals of $\boldsymbol{A}$, we may pose an equivalent lemma to Lemma 1.

Lemma 2 (Monotonicity on general grids in three dimensions)
The inverse of the matrix $\boldsymbol{A}$ generated from a 27-point discretization of the operator $[-\nabla\cdot(\boldsymbol{K}\nabla\bullet)]$ in two dimensions, on a general quadrilateral grid, is monotone if the following sufficient criteria are satisfied:

(E1): $\boldsymbol{A}_{2n+3}^{-1} \geq \boldsymbol{O}$.
(E2): $(\boldsymbol{A}\boldsymbol{A}_{2n+3}^{-1})$ *is an M-matrix.*

As in two dimensions, the computational cost is reduced with one order, for an $m \times n \times o$ grid from $O(m^2n^2o^2)$ to $O(m^2n^2o)$.

It is important to be aware that although these criteria have only been applied to MPFA methods, they are formulated to be applicable to any method which bases its approximation on a 9-point or 27-point stencil.

4.4 Monotonicity and the MPFA method

The Multi-Point Flux Approximation (MPFA) methods were introduced in [3]. For a thorough introduction to these methods, see [1] and references therein. A convergence proof for a specific method in two dimensions can be found in [39]. We will use the MPFA method to verify the monotonicity conditions (papers A and B), and also introduce a new class of MPFA discretization methods in Paper C.

We limit this introduction to MPFA discretizations in two dimensions. The building blocks of MPFA methods are approximations to fluxes over sub-interfaces . Referring to Figure 4.2, a sub-interface is the interface between a dividing point and the cluster center. In an interaction region, one assumes for purposes of calculating fluxes, that the pressure varies linearly in each

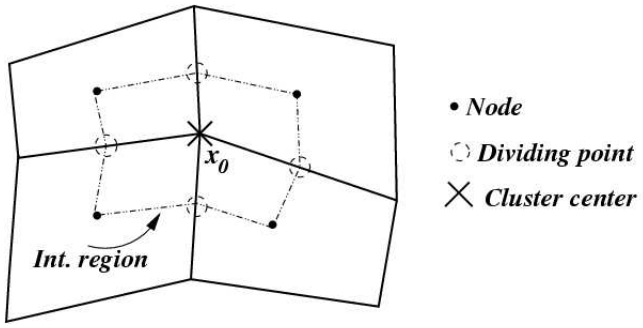

Figure 4.2: Four cells and their common interaction region

cell. Thus in each cell the pressure has three degrees of freedom. On logically Cartesian grids, four cells meet in a cluster center, hence the pressure approximation has 12 degrees of freedom in an interaction region.

The degrees of freedom are eliminated by 1) honoring cell center pressures, 2) imposing pressure continuity conditions along half edges, and 3) imposing flux continuity conditions over half edges. Since the pressure is approximated by piecewise linear functions, the fluxes may be evaluated analytically. Different choices of continuity conditions are termed O- and U- methods in literature based on different stylized shapes of the continuity conditions [2].

In this manner, half edge fluxes are determined, and subsequently assembled into cell stencils. A worked example of this procedure can be found for the O-method in [1], and for a new interaction region in Paper C.

To exemplify how the method varies with choice of continuity points, we will present some of the different coefficients m_i that appear for parallelogram grids. We describe the parallelogram grid by the vectors $\boldsymbol{a}_1$ and $\boldsymbol{a}_2$, which are normal to the surfaces of the parallelograms with length equal to the edge which they are normal to. With a homogenous permeability $\boldsymbol{K}$, we may define

$$a = \frac{1}{V}\boldsymbol{a}_1^T\boldsymbol{K}\boldsymbol{a}_1, \quad b = \frac{1}{V}\boldsymbol{a}_2^T\boldsymbol{K}\boldsymbol{a}_2, \quad c = \frac{1}{V}\boldsymbol{a}_1^T\boldsymbol{K}\boldsymbol{a}_2, \tag{4.15}$$

where V is the area (volume) of a cell. Then the coefficients for the O-method are [1]:

$$m_2 = -a + \frac{c^2}{d}, \quad m_3 = -\frac{c}{2} - \frac{c^2}{2d}, \quad m_4 = -b + \frac{c^2}{d}, \quad m_5 = \frac{c}{2} - \frac{c^2}{2d}, \tag{4.16}$$

where $d = 2ab/(a+b)$ is the harmonic mean of a and b. Due to symmetry,

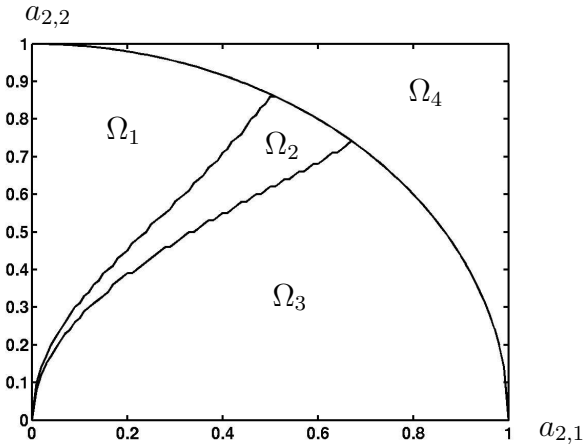

Figure 4.3: Comparison of analytical criteria and numerical results for the MPFA U-method.

$m_i = m_{i-4}$ for $5 \leq i \leq 9$. For the U-method these coefficients can be obtained:

$$m_2 = -a, \quad m_3 = -\frac{c}{2}, \quad m_4 = -b, \quad m_5 = \frac{c}{2}. \tag{4.17}$$

When the pressure continuity points are allowed to vary, similar expressions appear. In particular, with the choice of continuity points for the O-method used in [26], we get the coefficients

$$\begin{aligned} m_2 &= -\frac{5a}{8} + \frac{b}{8} + \frac{c^2}{d}, \quad m_3 = -\frac{3c}{8} - \frac{c^2}{4d} - \frac{ab}{8d}, \\ m_4 &= -\frac{5b}{8} + \frac{a}{8} + \frac{c^2}{d}, \quad m_5 = \frac{3c}{8} - \frac{c^2}{4d} - \frac{ab}{8d}. \end{aligned} \tag{4.18}$$

Observe that both the O- and U-methods with regular coefficients result in M-matrices only if $c = 0$; a condition which is termed $\boldsymbol{K}$-orthogonality. With the continuity points used in [26], we see that even for $\boldsymbol{K}$-orthogonal grids M-matrix properties are lost when the ratio $a/b > 5$ or $b/a > 5$. This implies that for aspect ratios more extreme than $1{:}\sqrt{5}$ on rectangular grids in homogenous media, the system matrix is not an M-matrix. Indeed, it turns out that the system matrix is not monotone either.

For all the coefficients in (4.16) – (4.18), good agreement is shown in Paper B between criteria C1 – C3 and actual monotonicity. Figure 4.3 shows a comparison using the MPFA U-method discretization. More examples are found in papers A and B. Every grid point in these figures represents the vector $\boldsymbol{a}_2 = [a_{2,1}, a_{2,2}]^T$, while the vector $\boldsymbol{a}_1 = [1, 0]^T$ is fixed. With this

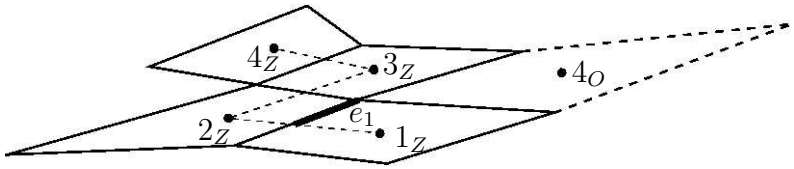

Figure 4.4: Interacting cells for Z-method

convention, Ω_1 is the domain where criteria C1 – C3 are satisfied, Ω_2 is where the criteria are not satisfied, but where we have no numerical example showing $\boldsymbol{A}^{-1} \ngeq \boldsymbol{O}$, while in Ω_3 we have examples showing $\boldsymbol{A}^{-1} \ngeq \boldsymbol{O}$. The domain Ω_4 is outside the unit circle, and may be disregarded since every point is symmetric to a point in Ω_1, Ω_2 or Ω_3.

In the preparations for this thesis, the O- and U-methods have been investigated for general choices of continuity points, extending the work in Paper B. New classes of MPFA methods combining continuity conditions from O- and U- methods were developed and investigated. For all investigated choices of continuity points and conditions, there was a significant set of $\boldsymbol{a}_2$ vectors where non-monotone behavior was observed. For practical purposes, the behavior for large aspect ratios in the grid are especially important. Note the asymptotic behavior of monotonicity, which places severe restrictions on grid skewness. This observation motivates the new interaction region introduced in Paper C. Before we proceed to irregular grids, this interaction region is presented.

4.5 The MPFA Z-method

While the interaction region in Figure 4.2 takes the four cells connecting in a cluster center as basis for the flux calculation, these four cells may not be the best suited. In Figure 4.4 we see an example where a fifth cell is closer to the cluster center than one of the connecting cells. We belive that this fifth point has important impact on flux over the interface, and that omitting it may be the cause for some of the monotonicity problems.

Focusing on sub-interface e_1 of Figure 4.4, an MPFA Z-method discretization approximates the flux across e_1 by a linear combination of the potentials in the cell nodes 1_Z through 4_Z. Classical MPFA methods would also use four potentials, however the point 4_O would be used instead of 4_Z. The coefficients of the four potentials is obtained by assuming pressure to vary linearly on each cell, and imposing flux and continuity conditions at the three internal surfaces of the interaction region. Details and a worked example for

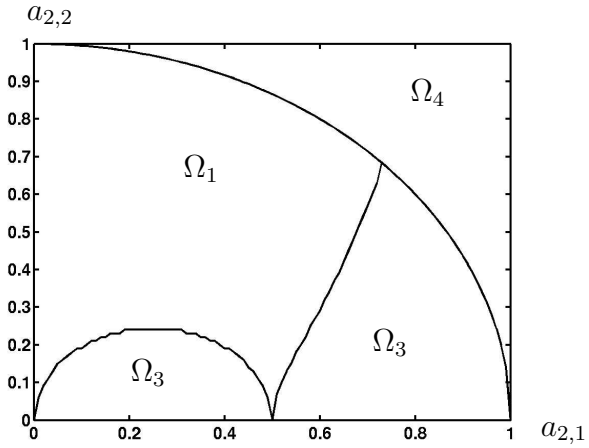

Figure 4.5: Comparison of analytical criteria and numerical results for the MPFA Z-method.

parallelogram grids can be found in Paper C. The coefficients that appear resemble those in equations (4.16) to (4.18),

$$m_2 = -a - c - \frac{c^2}{4a}, \quad m_4 = -b - c + \frac{c^2}{2a}, \quad m_5 = c + \frac{c^2}{2a}, \quad m_{16} = -\frac{c^2}{4a}. \tag{4.19}$$

Note the coefficient $m_{16}(= m_{24})$ corresponds to a cell outside the normal 9-point cell stencil. Further, coefficient m_3 is not used, such that the method remains a 9-point method for idealized grids. From symmetry and rotation we observe that there are four different Z-method discretizations of a parallelogram grid, the current one is intended for $c \leq 0$ and $a \leq b$.

In Paper C, both convergence and exact representation of linear flux is reported through examples, and the issue of monotonicity discussed. Since the MPFA Z-method is not a regular 9-point method, criteria C1-C3 are not applicable. However, investigation of the coefficients in (4.19) reveal that the Z-method has a large region where the discretization is an M-matrix. Figure 4.5 shows the M-matrix region, which for this method corresponds exactly to the numerical region of monotonicity (note that this figure represents a different rotation of the Z-method than the one in relations (4.19)). A comparison of the regions Ω_1 in figures 4.3 and 4.5 clearly show improved monotonicity properties for the Z-method in comparison with the U-method on parallelogram grids. The same result holds when comparing to the other MPFA discretizations. A comparison with the O-method with a resolved area around $|\boldsymbol{a_2}| < 0.1$ is included in Paper C.

4.6 Monotonicity on Quadrilateral Grids

Validating monotonicity criteria on general grids is more difficult than on homogeneous grids; a consequence of the fact that our variable space is larger, involving all possible logically Cartesian grids. Without attempting a full survey of this variable space, we investigate two sets of grids. The first set contains grids that are so distorted that Criterion D2 fails for all grids in the set. This set is used to evaluate the strength of Criterion D2c when applied to the O-method. A description of this set of grids and the experiments conducted can be found in Paper B. The second set, inspired by geometry from the Troll oil field, serves the purpose of comparing monotonicity properties of the MPFA Z-method with the commonly used O-method. This set was used in Paper C, which found that the Z-method handled skewed grids better than the O-method.

We conclude this section by summarizing the main findings. Paper A develops sufficient criteria for the monotonicity of the inverse matrix, applicable to any ordinary 9-point $\boldsymbol{K}$ method. This analysis is expanded in Paper B through a splitting of the system matrix. The analysis in Papers A and B motivates the development of a new MPFA method. Paper C introduces the MPFA Z-method, and shows improved monotonicity properties on both parallelogram and general quadrilateral grids. Uniform flow is reproduced, and a hybrid method consisting of both the O- and Z-method is used in a convergence example, where asymptotic 2nd order convergence is observed.

Chapter 5

Semi-Analytical Solutions

Leakage through abandoned wells may severely restrict the potential for geological sequestration of CO_2 in areas with significant oil exploration. This chapter investigates the possibility of obtaining analytical expressions for leakage through abandoned wells, such that the magnitude of leakage may easily be assessed. The main motivation for not using a numerical simulator is the need to simulate hundreds of wells with statistically known characteristics over long time spans. Accurate numerical simulations would require much grid refinement around wells, while our limited knowledge of well properties suggest that thousands of realizations will be desired. The computational effort needed to solve such problems numerically makes analytical solutions desirable.

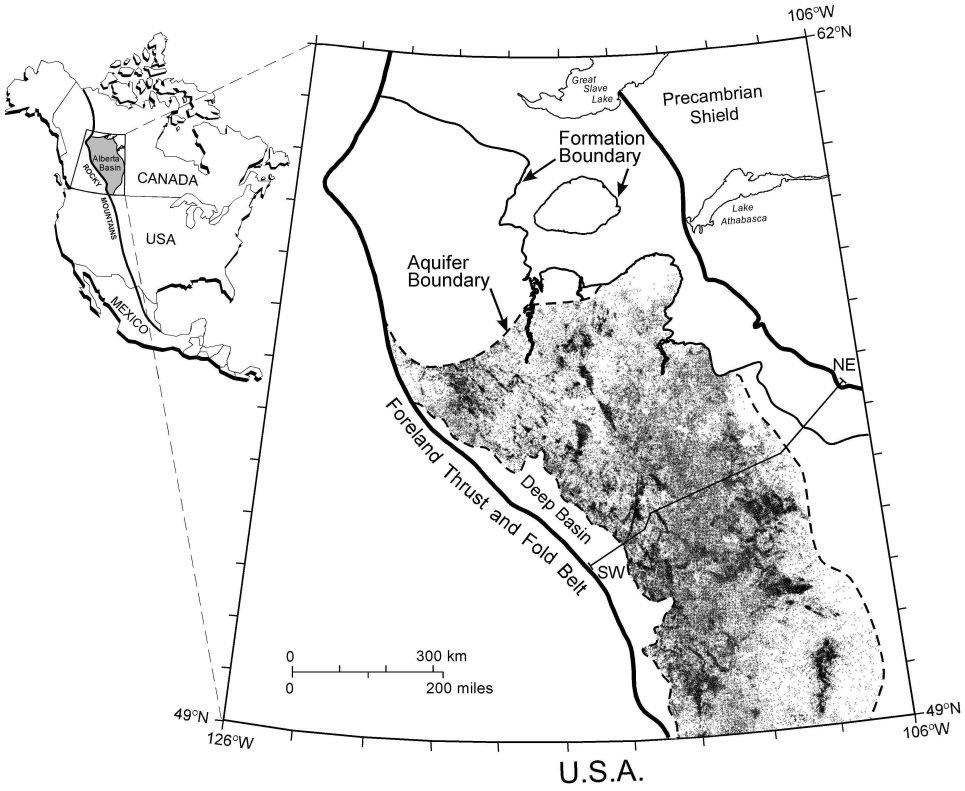

Figure 5.1: Location of wells in the Alberta Basin, every black dot represents a well (figure courtesy of the Alberta Geological Survey).

5.1 The Alberta Basin

In Alberta, restrictions on H_2S emissions have prompted injection activities into the underlying basin since 1989. Today there are 42 acid gas injection operations in the Alberta basin, where the injected gas is composed of 1% to 95% H_2S and 5% to 98% CO_2[10]. The injection sites are often located in areas with high levels of industry, often the same areas where there are many oil and gas wells.

Looking at all the wells drilled in Alberta, we see from Figure 5.1 that in certain areas the concentration of wells is extremely high, up to 25.8 wells per km^2 in areas associated with heavy oil production [34]. In regions associated with light oil and gas production, the density of wells is in the order of 1 to 10 wells per km^2 [34]. Approximately 60% of these wells are abandoned, implying that possible flow through these wells is not monitored and will not be detected. Most wells penetrate more than one formation,

such that abandoned wells provide connection not only between aquifers and the surface, but also amongst geologically separated formations.

For an injecting well, the radius of influence of the pressure perturbations caused by injection is typically several kilometers. Within this radius there may be literally hundreds of abandoned wells. If brine migrates upwards through these wells, there are at least four scenarios with negative impact [17]: Energy and natural resources in nearby formations may be affected; shallower groundwater resources (fresh water supplies) may be contaminated; leakage to the surface may have an effect on plants and wild life, as well as local inhabitants; injected waste may migrate all the way back to the atmosphere, reducing the effect of our sequestration efforts.

From this short review, it is clear that there is a need to asses the potential for leakage from acid gas and CO_2 injection operations, where there are large numbers of abandoned wells in the vicinity. Further, since only the location of these wells are known, and the permeability of the plugging will probably at best be known statistically, it is desirable to be able to run many realizations in a Monte Carlo setting. This emphasizes the need for developing methods which give fast an accurate solutions.

5.2 Governing Equations

We will start our investigation by considering the flow of a single fluid. When injecting into an infinite homogenous and horizontal aquifer with constant thickness, Equation (2.16) governs the flow. We will in this chapter assume that the aquifer permeability is isotropic, and that the aquifers are separated by impermeable layers (aquicludes). For simplicity, we assume that the viscosity is constant. Thus, the governing equation associated with injection can be written;

$$c\phi\frac{\partial}{\partial t}p - \frac{K}{\mu}\nabla^2 p = \frac{Q}{\rho_0}, \tag{5.1}$$

where p refers to a vertically averaged pressure (this can also be formulated by using hydraulic head, see Paper D for details). The source term on the right hand side includes all the active and abandoned wells in the domain. In the case of one vertical well, and one fluid (with constant viscosity μ, total fluid and porous compressibility c and density ρ), the solution to Equation (5.1) is given by Equation (2.17). This solution scales linearly with the injection rate, and we write

$$p(\boldsymbol{x}, t) - p_{init} = QW(\boldsymbol{x}, t). \tag{5.2}$$

Here the well function W is a function of the aquifer properties. Note that W has a slightly different definition in the papers. When the injection rate is dependent on time, we use the linearity of Equation (5.1) to superpose the change in injection rate. In the limit when the injection rate varies continuously, a convolution integral appears on the right hand side of Equation (5.2). Superposition is also valid when several wells are present. Combined, this yields a solution for arbitrary number of wells with varying discharge rates;

$$p(\boldsymbol{x}, t) - p_{init} = Q_0 W_0(\boldsymbol{x}, t) + \sum_{i=1}^{N} \left(\frac{\partial Q_i}{\partial t} * W_i \right) (\boldsymbol{x}, t). \tag{5.3}$$

We have numbered the wells such that wells 1 to N are abandoned, with unknown and varying flow rates, and well 0 is active with imposed constant flow rate. A single injecting well with constant injection rate, does not reduce generality, since additional injection wells and time varying rates can be superposed at a later stage. The binary operator $*$ refers to the convolution integral,

$$(f * g)(t) = \int_0^t f(\tau) g(t - \tau) d\tau = \int_0^t f(t - \tau) g(\tau) d\tau. \tag{5.4}$$

The abandoned wells are modeled as one-dimensional flow paths between neighboring aquifers in a layered sequence. We assume that no mass enters or leaves the well into the aquiclude. Abandoned wells are expected to be filled with cement or some other porous or solid medium, although the nature and properties of these variables are not yet fully surveyed. Therefore we choose to model flow in abandoned wells by a one-dimensional formulation of Darcy's law. Then the well flux is dependent on the pressures and the change in potential,

$$y = \frac{K_w \pi r_w^2}{\mu} \left(\frac{p_+ - p_-}{L} - \rho g \right). \tag{5.5}$$

The flow through the well is referred to as y, while subscripts $+$ and $-$ refer to the top and bottom of the well segment, respectively. The length and radius of the well are denoted L and r_w respectively, and the permeability K_w is the effective permeability of the well segment. The discharge Q_i into a layer equals the difference between the flow through the well segment directly above and below,

$$Q_i = y_{i+} - y_{i-}. \tag{5.6}$$

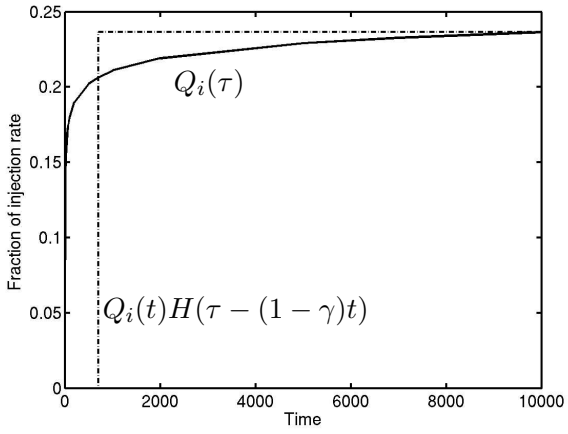

Figure 5.2: Leakage as a function of time compared to a Heaviside function. Leakage data from Avci [8].

With appropriate top and bottom boundary conditions, Equation (5.5) provides a coupling between the aquifers, and provides an expression for discharge rates from the abandoned wells.

Due to difficulties arising from the convolution operator, the system described by equations (5.3), (5.5) and (5.6) does not have an analytic solution, even in the simple case of two aquifers connected by one abandoned well. Avci does a Laplace transformation of the two aquifer, one well system, but winds up doing the inversion numerically [8]. None the less, we will refer to his solution in this simple case as the exact solution. Other semi-analytical and numerical solutions are discussed in Paper D.

5.3 Brine Leakage from Abandoned Wells

As noted, the main difficulty in the previous section arises from the convolution operator. In Paper D, it was proposed to approximate the convolution integral in Equation (5.3) using

$$\frac{\partial Q_i}{\partial t} * W_i(\boldsymbol{x}, t) \approx Q_i(t) W_i(\boldsymbol{x}, \gamma t). \tag{5.7}$$

This is equivalent to approximating $Q_i(\tau)$ by $Q_i(t)H(\tau - (1-\gamma)t)$ in the convolution integral, where H is the Heaviside function as shown in Figure 5.2. From the data presented by Avci [8], we observe that $Q_i(t)$ is monotone and increasing in the simplest case of one abandoned well. Thus the mean value theorem from calculus implies that there exists a $\gamma \in (0, 1)$ for which

Approximation (5.7) is exact. We will assume that $Q_i(t)$ is monotone also for more complex systems.

Assuming that γ is known, the governing equations reduce to a linear system, which may be solved directly for any given time. This is true independent of the number of abandoned wells and the number of aquifers in the system.

A comparison with the exact solution due to Avci [8] is carried out in Paper D. For all data given presented by Avci, $\gamma = 0.92$ provides a good approximation. Thus we hypothesize that γ is constant and equal to 0.92.

The exponential integral used in the well function W from Equation (2.17) can be difficult to evaluate. However, a series expansion of W is frequently used [11]:

$$\begin{aligned} W &= \frac{\mu}{4\pi K\rho_0}\int_u^\infty \frac{e^{-x}}{x}dx, \\ &= \frac{\mu}{4\pi K\rho_0}\left(-0.5772 - \ln u + u - \frac{u^2}{2\cdot 2!} + \frac{u^3}{3\cdot 3!}\dots\right). \end{aligned} \tag{5.8}$$

The variable u is given by Equation (2.17), and 0.5772 is Euler's (also referred to as Mascheroni's) constant. We see that for small u (indicating late times), the two first terms of the series expansion provides a good approximation to W. This is in fact the solution to the elliptic Equation (2.9), defined on a circular domain with a outer boundary moving at a velocity $v = C_R\sqrt{t}$, where C_r is a constant dependent on the compressibility, permeability and porosity. The moving outer boundary can be seen as an inclusion of compressibility in the incompressible elliptic equation through the boundary conditions. See Paper D for further details.

In Paper D the effect of approximating W by a truncated series expansion is investigated. Except at very early times, we may conclude that two terms are sufficient. Paper D further contains examples where multiple aquifer and multiple well systems are considered. Two main findings result from these examples.

In a multiple aquifer setup we investigate an injection aquifer roughly one kilometer below the surface, where the overlaying formation is either a solid impermeable aquiclude, or a set of 11 aquifers and aquicludes in succession upwards. While leakage out of the injection formation is lowest when the caprock consists of a single aquiclude, we find that leakage to the surface is several orders of magnitude lower when the overlaying formation consists of multiple aquifers and aquicludes. This effect is termed the elevator effect, as the leakage through abandoned wells are analogous to common experience

with hotel elevators; they are full when they leave the lobby and virtually empty as they reach the top floor.

In a multiple well experiment we place an increasing number of wells evenly spaced radially at a distance of 500 meters from the injection well. We observe that the increase in total leakage as a function of the number of wells is significantly less than linear, even when going from a single to two leaky wells placed on opposite sides of the injecting well.

5.4 CO_2 Plume Evolution

When more than one fluid is present, the complexity of the governing equations increases, as the positions of the fluids affect the flow properties and hence the pressure solution. Thus it is important to have knowledge of how the injected fluid flows through the aquifer.

To avoid dealing with dissolution and reaction rates, we assume that the fluids are immiscible and therefore non-reactant (CO_2 primarily enters reactions with formation minerals when dissolved in water [6]). Then flow is governed by the model described in Section 2.5. What we are interested in is the position of the interface between the CO_2 and brine during injection into an infinite aquifer. As far as the author knows, Equation (2.18) subject to (2.19) does not have an analytical solution in a homogeneous aquifer with three spacial dimensions with our boundary conditions. In the following we develop expressions for the interface between CO_2 and brine without actually solving Equation (2.18).

In Paper E two approximations to this interface are obtained. The first approximation is obtained using the numerical simulator ECLIPSE [53], which is a standard simulator used by the oil industry. However, a numerical solution does not fit in our analytical framework. The second approximation is obtained from the observation that the viscosity contrast between the fluids is far greater than the density contrast. This leads to the hypothesis that density merely serves the purpose of sorting the fluids vertically, while the shape of the plume itself is defined by the viscosity. We constrain the system based on an energy minimization argument. This is equivalent to requiring the pressure at the injection well to be at a minimum with respect to the distribution of CO_2. The well head pressure is calculated by solving an elliptic equation within a moving outer boundary, analog to the two-term truncated expansion used in the single-fluid case.

The two approximations fit well for four extreme cases of CO_2 injection described in Paper E. We see this as evidence that for conditions relevant to CO_2 injection, the depth b of the plume as a function of distance from

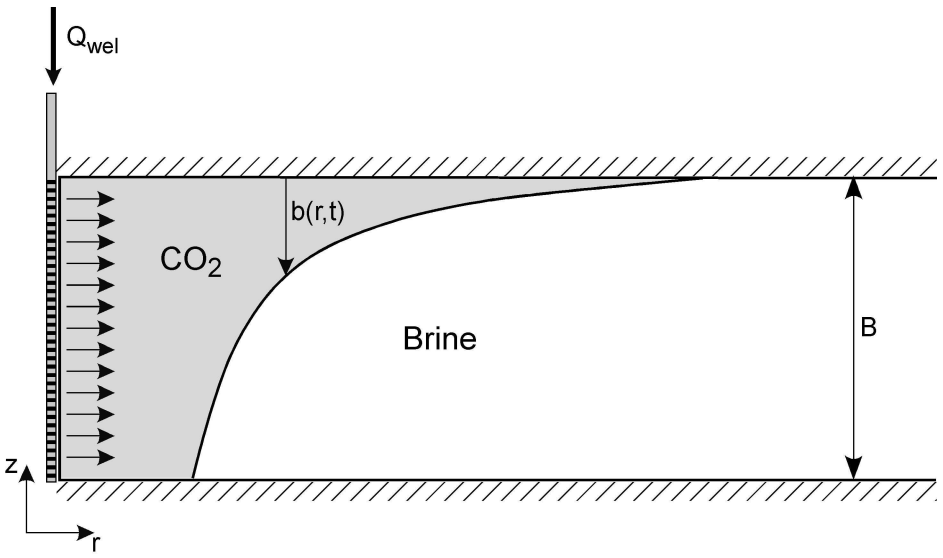

Figure 5.3: A cartoon showing the variables used for describing the CO_2 plume.

well r and time t (see Figure 5.3) can be approximated by the analytical approximation, which is given as

$$\frac{b(r,t)}{B} = \frac{1}{\lambda_c - \lambda_w}\left(\sqrt{\frac{\lambda_c \lambda_w A(t)}{\pi r^2}} - \lambda_w\right). \tag{5.9}$$

In this equation, mobility λ_i of fluid i is defined as the residual relative permeability over viscosity $k_{r,i}/\mu_i$, while B is the aquifer thickness. The areal factor A is equal to occupied volume divided by thickness, $AB = V = Qt/\phi$.

In Paper E the plume shape and Equation (5.9) were derived by approximating the plume by step functions and letting the number of steps go uniformly to infinity. This has the advantage that a stepwise approximation to the plume is a direct product of the derivation. Alternatively the expression in Equation (5.9) can be obtained through variational calculus, and for completeness, this is done here.

Let $\lambda = b\lambda_c + (B-b)\lambda_w$ be the vertically averaged mobility. Then replacing the parabolic Equation (2.18) by an elliptic equation as suggested by Equation (5.8), and ignoring the vertical dimension, the equation in a homogenous domain with constant fluid densities may be written

$$\begin{aligned} -K\nabla\cdot(\lambda\nabla p) &= \tfrac{Q}{\rho_0}, \\ p(|\boldsymbol{x}-\boldsymbol{x}_0|,t) = C_R\sqrt{t} &= R(t). \end{aligned} \tag{5.10}$$

The solution to this equation on a finite circular domain with injection in the center of the domain is

$$p(r,t) = -\frac{Q}{2\pi\rho_0 K}\int_{R(t)}^{r}\frac{dr}{r\lambda} = -\frac{Q}{2\pi\rho_0 K}\int_{R(t)}^{r}\frac{dr}{r(b(\lambda_c-\lambda_w)+B\lambda_w)}, \quad (5.11)$$

where $r = |\boldsymbol{x}-\boldsymbol{x}_0|$ is the distance from the injection. We want to minimize $p(r_0,t)$ subject to the volume constraint

$$-\int_{R}^{0} 2\pi b r dr = AB. \quad (5.12)$$

Denote the integrand of Equation (5.11) as $f(r,b)$ and the integrand of Equation (5.12) as $g(r,b)$. Then we know from variational calculus that when the well head pressure $p(r_0)$ is a minimum, $b(r)$ must satisfy

$$\frac{\partial(f+\Lambda g)}{\partial b} = 0. \quad (5.13)$$

Here Λ is a Lagrange multiplier. Solving Equation (5.13) for b yields

$$b(r,\Lambda) = \frac{B}{\lambda_c-\lambda_w}\left(\sqrt{\frac{\lambda_c-\lambda_w}{2\pi\Lambda r^2}}-\lambda_w\right). \quad (5.14)$$

We insert this expression into Equation (5.12) to obtain

$$\Lambda = \frac{\lambda_c-\lambda_w}{2\lambda_c\lambda_w A}. \quad (5.15)$$

Inserting Equation (5.15) into Equation (5.14) immediately yields Equation (5.9), and we conclude that the two approaches yield identical solutions.

5.5 CO_2 Leakage from Abandoned Wells

In Section 5.3 we observed that the solution of the parabolic equation can be approximated by an elliptic equation on a finite domain expanding with time. We further observed in Section 5.4 that the CO_2 plume evolution was dominated by viscous forces, and can be described by Equation (5.9). We combine these observations to obtain a simple solution to two-fluid leakage from abandoned wells.

The superposition used for single-fluid leakage does not apply when two fluids are present, since the operator

$$\mathcal{L}(u) = c\phi\frac{\partial u}{\partial t} - \nabla \cdot (K\lambda\nabla u) \tag{5.16}$$

is not constant in the space-time domain. However we recall that we could approximate the solution to the single-fluid problem by an elliptic problem for any time. Thus if we discretize the time dimension, the space operator

$$\mathcal{K}(u) = -\nabla \cdot (K\lambda\nabla u)) \tag{5.17}$$

is constant for each time step, and we may then use superposition.

Also, in the single-fluid case, it is not important if the brine leaking is resident or injected. With two-fluid injection, this becomes more important. Again, using time steps lets us keep track of where the fluids are and which fluids are leaking. The positions of the fluids feed back into the pressure solution, which gives the basis for leakage rates.

In Paper F, the ideas presented above are dealt with in detail. A solution algorithm is presented, which can be seen as an Implicit Pressure Explicit Saturation (IMPES) procedure:

i) Define the outer boundary as in the single-fluid problem, and solve for pressure based on the position of the fluids and well saturations from the previous time step.

ii) From the pressure solution and density properties, update the saturation in the wells.

iii) Determine leakage, and transport fluids according to the pressure solution, well saturations, and the plume shape from Equation (5.9).

iv) Repeat until desired time level.

This procedure is compared to output from ECLIPSE, and again we find good agreement between the simulated data and the analytical solution in respect to general behavior, and in particular leakage at late times. Two different functions for the well saturation are implemented, and we observe that the saturation in the well depends not only on the pressure difference between the aquifers, but also on variables such as the thickness of the plume at the well.

In summation, papers D through F develop analytical and semi-analytical solutions to well leakage problems of far greater complexity than found in the literature. The single-fluid solutions are generalized to arbitrary numbers of abandoned wells and time-dependent injecting wells, in geological systems with an arbitrary number of homogeneous aquifers. The two-fluid solutions

are limited to systems within which the fluid properties may be approximated as constant. The interaction of multiple plumes has not been studied, thus if more than one abandoned well is present the solution is limited in time since we do not have a model for leakage after the leakage plumes start merging. The two-fluid injection rate has so far been considered constant.

Chapter 6

Summary of Papers

There are six papers included in this thesis, of which five have been submitted for journal review, and one has been published in a conference proceedings. The papers can be divided into two groups, where papers A through C deal with the topics related to monotonicity presented in Chapter 4, while papers D through F deal with the analytic considerations presented in Chapter 5.

6.1 Paper A

J.M. Nordbotten and I. Aavatsmark, Monotonicity Conditions for Control Volume Methods on Uniform Parallelogram Grids in Homogeneous Media, submitted to *Computational Geosciences*

Abstract

Control volume methods are frequently used in porous media flow. This article gives an example on how one method, the Multi Point Flux Approximation method (MPFA), fails to satisfy the maximum principle for strong anisotropies or grid skewness, and develops conditions for when the maximum principle holds for uniform parallelogram grids in homogeneous media. The conditions developed are applicable to any nine-point scheme in 2D or 27-point scheme in 3D, and is useful when the method produces a system matrix which is not an M-matrix.

Main Results

- Criteria for non-monotone behavior for 9-point Control Volume methods on homogeneous parallelogram grids are obtained.
- The criteria are proved to be sufficient, though not necessary for monotone behavior.
- Application to the MPFA O-method shows that this method has a substantial region where the inverse operator is not monotone.
- Numerical validation shows that the criteria determine monotonicity correctly in the vast majority of the investigated cases.

6.2 Paper B

J.M. Nordbotten and G.T. Eigestad, Monotonicity Conditions for Control Volume Methods on General Quadrilateral Grids; Application to MPFA, *Proceedings of the 16. Nordic Seminar on Computational Mechanics*

Abstract

A novel approach to determining monotonicity of a Control Volume (CV) method on irregular, logically Cartesian grids in two dimensions is proposed. The choice of pressure and flux continuity constraints in the MPFA method are investigated in terms of monotonicity conditions.

Main Results

- Criteria for non-monotone behavior for Control Volume methods on general quadrilateral grids are obtained.
- The criteria are sufficient, though not necessary for monotone behavior.
- Application to the MPFA O-methods and U-methods shows that these methods have a substantial region where the inverse operator is not monotone. This result holds independent of the choice of continuity points.
- In Chapter 4 of this thesis the criteria in this paper are shown to be extensions of the criteria presented in Paper A.

6.3 Paper C

J.M. Nordbotten and G.T. Eigestad, Discretization on Quadrilateral Grids with Improved Monotonicity Properties, submitted to *Journal of Computational Physics*

Abstract

Monotonicity issues are known to arise for high aspect ratios combined with skewness of computational grids for Multi Point Flux Approximation (MPFA) methods. In this paper we improve the MPFA discretization techniques for general quadrilaterals, such that the above difficulties are handled to give a more robust discretization of the governing equations for fluid flow in porous media. Comparisons to the MPFA O-method are made, and the suggested discretization is shown to be an improvement in regards to monotonicity. For smooth solutions, the method performs equally well as the O-method when the convergence is examined.

Main Results

- A new MPFA discretization is introduced.
- The discretization yields M-matrices for a large set of parallelogram grids, thus expanding the region of inverse monotonicity.
- Exact reproduction of uniform flow is established.
- Combined with the MPFA O-method, the new method displays asymptotic second order convergence for a numerical example.
- The MPFA Z-method is shown to perform better than the O-method in experiments on general quadrilateral grids.

6.4 Paper D

J.M. Nordbotten, M.A. Celia and S. Bachu, Analytical Solutions for Leakage Rates Through Abandoned Wells, submitted to *Water Resources Research*

Abstract

Disposal of waste fluids via injection into deep saline aquifers is practiced in a variety of industries. Injection takes place in sedimentary basins that often have a history of oil and gas exploration and production, which means that wells other than those used for waste disposal may exist in the vicinity of the injection site. These existing wells provide possible pathways for leakage of waste fluids toward the shallow subsurface and the land surface. For single-phase flows of liquids with essentially constant properties, the equations governing the system are linear, and solutions may be written using the superposition principle. Because leakage through existing wells produces a time-varying flux rate, the solution of the governing equations involves convolution integrals. Previous solutions have addressed the problem of one injection well, one existing (passive) well, and a simple geometry of two aquifers separated by an aquitard by use of Laplace transforms. Even for this simple case, inversion of the transform is difficult. Solutions involving more than one passive well have not been developed. Nor have solutions been developed for more than two aquifers and one aquitard. Realistic injection cases often involve layered systems with multiple aquifers and aquitards, as well as multiple passive wells, sometimes numbering in the hundreds. Solutions for the general case of multiple aquifers and wells may be developed through introduction of approximations to the well function, and appropriate simplification of the convolution integral. Such a solution is computationally simple. Comparison to solutions using the full (Laplace transform) solution indicates that the new solution procedure produces excellent results. Application of the new solution to a case of multiple passive wells shows that the cumulative leakage flux in the passive wells is not a simple sum of the single-well case, owing to leakage-induced drawdown around the passive wells. In addition, application to the case of multiple aquifers and aquitards demonstrates the importance of leakage into intervening aquifers as a mechanism to

mitigate leakage into shallow zones, a process referred to as the 'elevator model'. The new analytical solution provides a tool to analyze practical injection problems, and forms a foundation on which more complex solutions, such as those involving injection of a non-aqueous fluid into a deep brine formation, may be based.

Main Results

- A novel solution for well leakage is presented.
- The new solution is shown to reproduce results from previously solved problems.
- The solution extends to problems which previously have not been solved, namely arbitrary numbers of wells and aquifers.
- The computational cost is very low; a single linear set of [number of wells]$\times$[number of aquifers] equations expresses abandoned well leakage rates at any given time.

6.5 Paper E

J.M. Nordbotten, M.A. Celia and S. Bachu, Injection and Storage of CO_2 in Deep Saline Aquifers: Analytical Solution for CO_2 Plume Evolution During Injection, submitted to *Transport in Porous Media*

Abstract

Injection of fluids into deep saline aquifers is practiced in several industrial activities, and is being considered as part of a possible mitigation strategy to reduce anthropogenic emissions of carbon dioxide into the atmosphere. Injection of CO_2 into deep saline aquifers involves CO_2 as a supercritical fluid that is less dense and less viscous than the resident formation water. These fluid properties lead to gravity override and possible viscous fingering. With relatively mild assumptions regarding fluid properties and displacement patterns, an analytical solution may be derived to describe the space-time evolution of the CO_2 plume. The solution assumes a sharp interface between the two fluids, and provides simple closed-form expressions for the temporal evolution of the interface in both the radial and the vertical directions. In order to test the applicability of the analytical solution to the CO_2 injection problem, we consider a wide range of subsurface conditions, characteristic of sedimentary basins around the world, that are expected to apply to possible CO_2 injection scenarios. For comparison, we run numerical simulations with an industry standard simulator, and show that the new analytical solution matches a full numerical solution for the entire range of CO_2 injection scenarios. The new analytical solution is remarkably simple, and provides a tool to estimate practical quantities associated with CO_2 injection, including maximum spatial extent of a plume and the shape of the overriding less dense CO_2 front.

Main Results

- Based on principles of minimization of work, a plume shape is found analytically.

- The analytical plume is shown to fit with four representative viscosity and density sets associated with CO_2 injection.
- Knowledge of the evolution of the CO_2 plume will facilitate the development of analytical solutions to two-fluid flow within the framework presented in Paper D.

6.6 Paper F

J.M. Nordbotten, M.A. Celia, S. Bachu and H.K. Dahle, Semi-Analytical Solution for CO_2 Leakage through an Abandoned Well, submitted to *Environmental Science & Technology*

Abstract

Capture and subsequent injection of carbon dioxide into deep geological formations is being considered as a means to reduce anthropogenic emissions of CO_2 to the atmosphere. If such a strategy is to be successful, the injected CO_2 must remain within the injection formation for long periods of time, at least several hundred years. Because mature continental sedimentary basins have a century-long history of oil and gas exploration and production, they are characterized by large numbers of existing oil and gas wells. For example, more than a million such wells have been drilled in the state of Texas, in the United States. These existing wells represent potential leakage pathways for injected CO_2. In order to analyze leakage potential, modeling tools are needed to predict leakage rates and patterns in systems with injection and potentially leaky wells. We have developed a semi-analytical solution framework that predicts leakage rates for the case of injection of supercritical CO_2 into a brine-saturated deep aquifer, taking into account both density and viscosity differences between the two fluids. The solution predicts the extent of the injected CO_2 plume, as well as the evolving pressure field, within the injection formation. It also provides leakage rates through a leaky well located at an arbitrary distance from the injection well, along with the solution for the spatial distribution CO_2 and the pressure field in the overlying aquifer into which the CO_2 leaks. Results from a full multi-phase flow simulator show excellent agreement with the new semi-analytical solution. Example calculations also show the importance of outer boundary conditions, and the influence of both density and viscosity contrasts in the resulting solutions. The new semi-analytical solution provides a simple and efficient procedure for leakage estimation for problems involving one injection well, one leaky well, and two aquifers separated by an impermeable aquitard.

Main Results

- A model for leakage through abandoned wells in scenarios with two fluids is presented.
- A comparison to a numerical simulator shows good agreement between the analytical leakage and leakage predicted by conventional numerical means.
- Cases are presented which show the effect of viscosity and density on leakage, and the leakage is seen to reduce to single-fluid leakage when the fluids have equal properties.

Chapter 7

Further Research

In this thesis we have focused on two main ideas; investigating monotonicity properties of Control Volume 9-point discretizations, and developing analytical solutions for single- and two-fluid well leakage. We will here outline some of the research questions that arise from the work contained in this thesis.

7.1 Monotone Discrete Operators

We have studied the properties of discrete representations of the incompressible pressure equation, in particular we were concerned with monotonicity. This lead to direct criteria on the elements of the system matrix in the case of parallelogram grids. For more general grids a matrix splitting was introduced that leads to fast and reliable monotonicity conditions. Application of these monotonicity studies motivated the development of a new MPFA method, the Z-method. In numerical examples, the Z-method retains the same convergence rate as the MPFA O-method, while significantly improved results are observed in respect to monotonicity, both in homogeneous and heterogeneous media.

Future research within this subject should consider obtaining complimentary results to those presented here. Thus since we give sufficient criteria that the inverse operator is monotone, the complimentary question is if there are criteria for when the inverse operator is non-monotone.

Some results have been stated for three dimensions, these have not been investigated. While they are sufficient criteria, they may be too restrictive to be of any practical interest. Also, application of the monotonicity criteria, to the Z-method still remains to be done.

The Z-method is also described and tested in two dimensions. While the extension to three dimension is straight forward, this has not been implemented. Convergence results are given for one grid, a more detailed study of convergence is desired.

Further, regular MPFA U- and O-discretizations result in banded system matrices with 9 and 27 diagonal bands in two and three dimensions respectively. As the Z-method does not use fixed interaction regions, the system matrices will contain additional bands. The effect this has on computational cost needs to be assessed before implementation in simulators.

7.2 Leakage from Abandoned Wells

Our development of expressions for well leakage has been fruitful. We now have direct expressions for leakage from single-fluid systems containing an arbitrary number of aquifers and wells, both injecting and abandoned. For two-fluid systems, we have obtained an expression for the CO_2 plume, which is valid for a wide range of injection conditions. This expression has been combined with the methodology of single-fluid leakage, and a semi-analytical expression for leakage of CO_2 from abandoned wells has been obtained.

Our single-fluid solution does not yet consider aquifers separated by per-

meable aquitards. Also, our approximation of the convolution integral has not been investigated in the presence of more than one abandoned well. These are topics on which work is ongoing.

The study of two-fluid leakage still has many questions which require answers. We are limited to problems where the density change of the CO_2 is small, which puts a restriction on the vertical migration that we can consider. We are not yet able to solve systems where CO_2 plumes interact with each other, which limits the placement of abandoned wells. Evolution of the CO_2 plume after injection shutoff, or more generally, when the injection rate is varying, is not known. It is important for application that the methods presented here are extended to overcome these challenges. Effects such as capillary pressure, aquitard permeability, sloping aquifers, and phase transitions are other topics that have not yet been investigated.

Of a more computational nature is an inclusion of adaptive time stepping. While the current implementation uses constant time steps, it seems natural that refinement in time is only needed when the CO_2 front passes abandoned wells, or when CO_2 plumes start interacting.

The work contained in this thesis gives a new approach to modeling two-fluid flow, in particular in our application of leakage through abandoned wells. This section highlights that although good results have already been obtained, there are significant challenges ahead before a full description of the system has been obtained.

Bibliography

[1] I. Aavatsmark. An introduction to multipoint flux approximations for quadrilateral grids. *Computational Geosciences*, 6:405–432, 2002.

[2] I. Aavatsmark, T. Barkve, . Be, and T. Mannseth. A class of discretization methods for structured and unstructured grids in anisotropic, inhomogeneous media. *Proceedings of the 5th European conference on the mathematics of oil recovery*, 1996.

[3] I. Aavatsmark, T. Barkve, Ø. Bøe, and T. Mannseth. Discretization on non-orthogonal, curvilinear grids for multi-phase flow. *Proceedings of the 4th European Conference on the Mathematics of Oil Recovery*, 1994.

[4] J.J. Adams and S. Bachu. Equations of state for basin geofluids: Algorithm review and intercomparison for brines. *Geofluids*, 2002.

[5] D.L. Albritton and L.G. Meira Filho. Climate change 2001: The scientific basis; Contribution of working group i to the third assessment report of the ipcc - Technical summary. *IPCC: Geneva, Switzerland*, 2001.

[6] C.A.J Appelo and D. Postma. *Geochemistry, groundwater and pollution*. A.A. Balkema, 1999.

[7] T. Arbogast, M.F. Wheeler, and I. Yotov. Enhanced cell-centered finite differences for elliptic equations on general geometry. *SIAM Journal of Scientific Computing*, 19:404–425, 1998.

[8] C.B. Avci. Evaluation of flow leakage through abandoned wells and boreholes. *Water Resources Research*, 1994.

[9] S. Bachu and J.J. Adams. Sequestration of CO_2 in geological media in response to climate change: capacity of deep saline aquifers to sequester CO_2 in solution. *Energy Conversion and Management*, 2003.

[10] S. Bachu and W.D. Gunther. Acid gas injection in the Alberta basin, Canada; a CO_2 storage experience. In S.J. Baines and R.H. Worden, editors, *Geological Storage of Carbon Dioxide for Emissions Reduction: Technology*. Geological Society Special Publication, Bath, U.K. In press.

[11] J. Bear. *Hydraulics of Groundwater*. McGraw-Hill, 1979.

[12] A. Berman and R.J. Plemmons. *Nonnegative Matrices in the Mathematical Sciences*. Academic Press, New York, 1979.

[13] M.J. Blunt, M.D. Jackson, M. Piri, and P.H. Valvatne. Detailed physics, predictive capabilities and macroscopic consequences for pore-network models of multiphase flow. *Advances in Water Resources*, 25(8-12):1069–1089, 2002.

[14] D. Braess. *Finite Elements*. Cambridge University Press, 1997.

[15] F. Brezzi and M. Fortin. *Mixed and Hybrid Finite Element Methods*, volume 15 of *Springer Series in Computational Mathematics*. Springer-Verlag, New York, 1991.

[16] R.G. Bruant, A.J. Guswa, M.A. Celia, and C.A. Peters. Safe storage of CO_2 in deep saline aquifers. *Environmental Science and Technology*, June 2002.

[17] M.A. Celia and S. Bachu. Geological sequestration of CO_2: is leakage unavoidable and acceptable? *Proceedings of the Sixth International Greenhouse Gas Technologies Conference*, 2002.

[18] M. Chaib. *Implicit Molar Mass Formulations in Secondary Oil Migration*. PhD thesis, University of Bergen, 2002.

[19] Q. Chen, W. Kinzelbach, C. Ye, and Y. Yue. Variations of permeability and pore size distribution of porous media with pressure. *Journal of Environmental Quality*, 31:500–505, 2002.

[20] H. Class, R. Helmig, and P. Bastian. Numerical simulation of non-isothermal multiphase multicomponent processes in porous media. 1. An efficient solution technique. *Advances in Water Resources*, 25:533–550, 2002.

[21] H. Class and R. Helmig. Numerical simulation of non-isothermal multiphase multicomponent processes in porous media. 2. Applications

for the injection of steam and air. *Advances in Water Resources*, 25:551–564, 2002.

[22] B.S. Cole. An equation of state for multiphase CO_2 and water. Master's thesis, New Mexico Institute of Mining and Technology, 1999.

[23] S.D. Conte and C. de Boor. *Elementary Numerical Analysis*. McGraw-Hill, 1981.

[24] H. Darcy. *Les fontaines publiques de la ville Dijon*, pages 590–594. Victor Dalmont, Paris, 1856.

[25] F.A.L. Dullien. *Porous Media Fluid Transport and Pore Structure*. Academic Press, 1979.

[26] M. Edwards. Finite volume discretization with imposed flux continuity for the general tensor pressure equation. *Computational Geosciences*, 2:259–290, 1998.

[27] M.G Edwards, R.G. Lazarov, and I. Yotov, editors. *Special Issue on Locally Conservative Methods for Flow in Porous Media*, volume 6. Computational Geosciences, 2002.

[28] M.S. Espedal and K.H. Karlsen. Numerical solution of reservoir flow models based on large time step operator splitting algorithms. *Lecture Notes in Mathematics*, 1734, 1998.

[29] L.C. Evans. *Partial Differential Equations*. American Mathematical Society, 1998.

[30] G.E. Fladmark. *Secondary Oil Migration; Mathematical and numerical model.* Lecture notes, 1997.

[31] G.E. Fladmark. *User manual for SOMXXX A secondary hydrocarbon migration simulator*, 2001.

[32] P. Fletcher. *Chemical Thermodynamics for Earth Scientists*. Longman Scientific and Technical, 1993.

[33] R.A. Freeze and J.A. Cherry. *Groundwater*. Prentice Hall, 1979.

[34] S.E Gasda, S. Bachu, and M.A. Celia. Spatial characterization of existing well locations in a mature sedimentary basin. *Environmental Geology*, 2003. Submitted.

[35] W. Hackbusch. *Theorie und Numerik elliptischer Differentialgleichungen*. Teubner, Stuttgart, 1986. English translation (Springer-Verlag, Berlin, 1992).

[36] J. T. Houghton, Y. Ding, D.J. Griggs, M. Noguer, and P. J. van der Linden, editors. *Climate Change 2001: The Scientific Basis*. Cambridge University Press, 2001.

[37] B. Hunt. Flow to a well in a multiaquifer system. *Water Resources Research*, 21(11):1637–1641, 1985.

[38] J. Hyman, M. Shashkov, and S. Steinberg. The numerical solution of diffusion problems in strongly heterogeneous non-isotropic materials. *Journal of Computational Physics*, 132:130–148, 1997.

[39] R.A. Klausen. Convergence of multi-point flux approximations on quadrilateral grids. 2004.

[40] R.A. Klausen and T.F. Russell. Relationships among some locally conservative discretization methods which handle discontinuous coefficients. 2004.

[41] B.P. McGrail, M.D. White, P.F. Martin, and H.T. Schaef. Mixing rates of supercritical CO_2 with brine in deep sedimentary formations. *Proceedings of the Second Annual Conference on Carbon Sequestration*, 2003.

[42] Miljø 2003; Petroleumsektoren i Norge. *Olje- og energidepartementet*, 2003. In Norwegian.

[43] J.M. Nordbotten. Store problemer, dype løsninger. *AKA*, (9), 2003. Special issue on human interactions with nature, In Norwegian.

[44] Norwegian Petroleum Directorate. http://www.npd.no/.

[45] E. Øyan, I. Garrido, M. Chaib, G. Fladmark, and M. Espedal. Modeling fractured and faulted regions: Local grid refinement methods for implicit solvers. *Computing and Visualization in Science*, 2003. accepted.

[46] G. Øye. *An Object-Oriented Parallel Implementation of local Grid Refinement and Domain Decomposition in a Simulator for Secondary Oil Migration*. PhD thesis, University of Bergen, 1999.

[47] M. Quintard and S. Whitaker. Two-phase flow in heterogeneous porous media: The method of large-scale averaging. *Transport in Porous Media*, 1988.

[48] H. Reme. *The Preconditioning and Multi Point Flux Approximation Methods for solving Secondary Oil Migration and Upscaling Problems.* PhD thesis, University of Bergen, 1999.

[49] T.F. Russell. Relationships among some conservative discretization methods. *Lecture Notes in Physics*, pages 1–16, 1999.

[50] The SACS project. http://www.iku.sintef.no/projects/IK23430000/.

[51] M. Shashkov. *Conservative Finite-Difference Methods on General Grids.* CRC Press, 1996.

[52] M. Shashkov and S. Steinberg. Solving diffusion equations with rough coefficients in rough grids. *Journal of Computational Physics*, 129:383–405, 1996.

[53] Eclipse technical description. Schlumberger Information Solutions, 2002.

[54] R. Span and R. Wagner. A new equation of state for carbon dioxide covering the fluid region from the triple-point temperature to 100 K at pressures up to 800 MPa. *Journal of Physical and Chemical Reference Data*, 1996.

[55] C.V. Theis. The relationship between the lowering of the piezometric surface and the rate and duration of discharge of a well using ground-water storage. *American Geophysical Union Transactions*, 16:519–524, 1935.

[56] *Second Annual Conference on Carbon Sequestration.* US Department of Energy, 2003.

Part II

Note: The original thesis contained preprints of the following papers. In order to observe copy-right, and to preserve a notion of a definite version of the works, these preprints have been omitted in this file. Interested readers may find are referred to the references indicated below.

Jan Martin Nordbotten,
Princeton, September 2005

Bibliography

[Paper A] J. M. Nordbotten and I. Aavatsmark. Monotonicity conditions for control volume methods on uniform parallelogram grids in homogeneous media. *Computational Geosciences*, 9(1):61-72, 2005.

[Paper B] J. M. Nordbotten and G. T. Eigestad. Monotonicity conditions for control volume methods on general quadrilateral grids; Application to MPFA. *Proceedings of the 16th Nordic Seminar on Computational Mechanics*, 16. Oct. 2003.

[Paper C] J. M. Nordbotten and G. T. Eigestad. Discretization on quadrilateral grids with improved monotonicity properties. *Journal of Computational Physics*, 203(2):744–760, 2004.

[Paper D] J. M. Nordbotten, M. A. Celia, and S. Bachu. Analytical solutions for leakage rates through abandoned wells. *Water Resources Research*, 40(4):W04204, 2004.

[Paper E] J. M. Nordbotten, M. A. Celia, and S. Bachu. Injection and storage of CO_2 in deep saline aquifers: Analytical solution for CO_2 plume evolution during injection. *Transport in Porous Media*, 58(3):339–360, 2005.

[Paper F] J. M. Nordbotten, M. A. Celia, S. Bachu, and H. K. Dahle. Semi-analytical solution for CO_2 leakage through an abandoned well. *Environmental Science and Technology*, 39(2):602–611, 2005.